Eur. Phys. J. C 9, 463–477 (1999)
DOI 10.1007/s100529900027

THE EUROPEAN PHYSICAL JOURNAL C


# Top-quark pair production via polarized and unpolarized protons in the supersymmetric QCD*

Yu Zeng-Hui[1,3], Herbert Pietschmann[1], Ma Wen-Gan[2,3], Han Liang[3], Jiang Yi[3]

[1] Institut für Theoretische Physik, Universität Wien, A-1090 Vienna, Austria
[2] CCAST (World Laboratory), P.O. Box 8730, Beijing 100080, P.R. China
[3] Department of Modern Physics, University of Science and Technology of China (USTC), Hefei, Anhui 230027, P.R. China

Received: 30 September 1998 / Revised version: 21 January 1999 / Published online: 28 May 1999

**Abstract.** The QCD corrections to the top-quark pair production via both polarized and unpolarized gluon fusion in $pp$ collisions are calculated in the minimal supersymmetric model (MSSM). We find that the MSSM QCD corrections can reach 4% and may be observable in future precise experiments. Furthermore, we studied CP violation in the MSSM. Our results show that the CP-violating parameter is sensitive to the masses of SUSY particles (it becomes zero when the c.m. energy is less than twice the masses of both the gluino and the stop quarks) and may reach $10^{-3}$.

## 1 Introduction

The minimal supersymmetric model (MSSM) [1] is one of the most interesting extensions of the standard model (SM). Therefore, testing the MSSM has attracted much interest. As is well known, the MSSM predicts supersymmetric (SUSY) partners to all particles expected by the SM, and searching for their existence is very important.

Since the top quark was already found experimentally by the CDF and D0 Collaborations at Fermilab [2], we believe that more experimental events including the top quark will be collected in future experiments. That gives us a good chance to study the physics in top-quark pair production from $pp$ or $p\bar{p}$ collisions with more precise experimental results. Because of the heavy mass of the top quark, this process provides a test of the SM and possible signals of new physics at high energy.

The dominant subprocesses of top-quark pair production in $pp$ or $p\bar{p}$ colliders are quark–antiquark annihilation and gluon–gluon fusion. The lowest order of those two subprocesses has been studied in [3]. There it was found that the former subprocess ($q\bar{q}$ annihilation) is more dominant in $p\bar{p}$ collisions when the c.m. energy ($\sqrt{s}$) is near the threshold value $2m_t$, whereas the subprocess via $gg$ fusion will become increasingly important with increasing c.m. energy, and can become the most dominant process when the c.m. energy is much larger than $2m_t$.

In [4], the QCD corrections to top-quark pair production in $p\bar{p}$ collisions have been studied in the frame of the SM. It may seem natural that the QCD corrections of those processes in the frame of the MSSM are important for distinguishing those two models. Recently, the SUSY QCD corrections to top-pair production via $q\bar{q}$ annihilation were presented [5]. The SUSY QCD corrections via unpolarized gluon–gluon fusion were given by Li et al. [6].

It is obvious that the correction from the SUSY QCD is related to the masses of the top quark and of SUSY particles. Assuming the SUSY breaking scale to be at about 1 TeV, the masses of SUSY particles would be smaller than 1 TeV. Therefore we can hope that corrections from SUSY particles are significant, since the heavy mass of the top quark ($m_t = 175.6 \pm 5.5\,\mathrm{GeV}$ (world average)) may be comparable to some of the light SUSY particle masses. Therefore the SUSY QCD correction would indirectly give us some significant information about the existence of SUSY particles.

Recently, the spin structure of the nucleon has been intensively studied by polarized deep-inelastic-scattering experiments at CERN and SLAC. Knowledge about this allows us to find a clear signal beyond the SM, if we collect enough events in the process of top-quark pair production from polarized $pp$ or $p\bar{p}$ collisions. In the SM QCD there is no CP-violation mechanism, whereas in the SUSY QCD the situation may be different. If we introduce a phase angle of quark SUSY partners, we can get CP violation in the MSSM QCD [7]. Once we get enough statistics of top-quark pairs from $pp$ or $p\bar{p}$ colliders at higher energy, it will be possible to test CP violation. On the other hand, the spin-dependent parton distributions can be obtained from their polarized structure function data given in [8, 10,11]. There it is found that the shape of polarized gluon and quark distributions in the nucleon depends on its polarization. Therefore the CP-violation effects through the

* Supported in part by a Committee of the National Natural Science Foundation of China and Project IV.B.12 of a scientific and technological cooperation agreement between China and Austria.

process of top-quark pair production via $gg$ fusion may be observed in polarized $pp$ or $p\bar{p}$ collisions.

In this work we concentrate on the SUSY QCD corrections to the process $pp \to gg \to t\bar{t}X$ both in polarized and unpolarized colliding beams. In Sect. 2 we give the tree-level contribution to the subprocess $gg \to t\bar{t}$. In Sect. 3 we give the analytical expressions of the SUSY QCD corrections to $gg \to t\bar{t}$. In Sect. 4 the numerical results of the subprocess $gg \to t\bar{t}$ and the process $pp \to gg \to t\bar{t}X$ are presented. The conclusion is given in Sect. 5, and some details of the expressions are listed in the Appendix.

## 2 The tree-level subprocess

The graphical representation of the process $g(\lambda_1, k_1)$ $g(\lambda_2, k_2) \to t(p_1)\bar{t}(p_2)$ is shown in Fig. 1a. The Mandelstam variables are defined as usual:

$$\hat{s} = (p_1 + p_2)^2 = (k_1 + k_2)^2, \tag{2.1}$$

$$\hat{t} = (p_1 - k_1)^2 = (k_2 - p_2)^2, \tag{2.2}$$

$$\hat{u} = (p_1 - k_2)^2 = (k_1 - p_2)^2, \tag{2.3}$$

so $\hat{s} + \hat{t} + \hat{u} = 2m_t^2$. The amplitude of tree-level diagrams with polarized gluons can be written as in [3] ($a, b$ are color indices of external gluons, $i, j$ are colors of external top quarks, and $T^a = \lambda_a/2$ are the Gell-Mann matrices):

$$M_0^{(l)} = g_s^2 \epsilon^{\mu,a}(\lambda_1, k_1)\epsilon^{\nu,b}(\lambda_2, k_2)\bar{u}_i(p_1)\Gamma^{(l)}v_j(p_2), \quad (l = s, t, u), \tag{2.4}$$

with

$$\Gamma^{(s)} = \frac{T^c_{ij} f_{abc}}{s}[(\not{k}_1 - \not{k}_2)g_{\mu\nu} + (2k_2 + k_1)_\mu \gamma_\nu - (2k_1 + k_2)_\nu \gamma_\mu], \tag{2.5}$$

$$\Gamma^{(t)} = \frac{-\mathrm{i}T^a_{im}T^b_{mj}}{t - m_t^2}\gamma_\mu(\not{k}_2 - \not{p}_2 + m_t)\gamma_\nu, \tag{2.6}$$

$$\Gamma^{(u)} = \frac{-\mathrm{i}T^b_{im}T^a_{mj}}{u - m_t^2}\gamma_\nu(\not{k}_1 - \not{p}_2 + m_t)\gamma_\mu. \tag{2.7}$$

We chose a form in which only physical polarizations of gluons remained:

$$\epsilon^{\mu*}(\lambda_1, k_i)\epsilon^{\nu}(\lambda_2, k_i) = \frac{\delta_{\lambda_1,\lambda_2}}{2}\left(-g^{\mu\nu} + \frac{n^\mu k_i^\nu + n^\nu k_i^\mu}{n \cdot k_i} - \frac{n^2 k_i^\mu k_i^\nu}{(n \cdot k_i)^2} + \mathrm{i}\lambda_1 \epsilon^{\sigma\mu\rho\nu}\frac{k_{i\sigma}n_\rho}{n \cdot k_i}\right), \tag{2.8}$$

where $n = k_1 + k_2$ and $\lambda_{1,2} = \pm 1$. From that we can get the cross section at the tree level with both polarized and unpolarized gluons.

## 3 SUSY QCD corrections (non-SM) to the subprocess $gg \to t\bar{t}$

### 3.1 Relevant Lagrangian in the MSSM

The difference between the MSSM QCD and the SM QCD corrections stems from the interactions of SUSY particles. Thus we can divide SUSY QCD corrections into a standard and a non-standard part. The Lagrangian density of the non-SM part of the SUSY QCD interaction is written as:

$$L = L_1 + L_2 + L_3 + L_4, \tag{3.1.1}$$

where

$$L_1 = -\mathrm{i}g_s A_a^\mu T^a_{jk}(\tilde{q}^j_{\mathrm{L}}\partial_\mu \tilde{q}^k_{\mathrm{L}} - \tilde{q}^k_{\mathrm{L}}\partial_\mu \tilde{q}^j_{\mathrm{L}}) + (\mathrm{L} \to \mathrm{R}), \tag{3.1.2}$$

$$L_2 = -\sqrt{2}\hat{g}_s T^a_{jk}(\bar{\tilde{g}}_a P_{\mathrm{L}} q^k \tilde{q}^{j*}_{\mathrm{L}} + \tilde{q}^j P_{\mathrm{R}} \tilde{g}_a \tilde{q}^k_{\mathrm{L}} - \bar{\tilde{g}}_a P_{\mathrm{R}} q^k \tilde{q}^{j*}_{\mathrm{R}} - \bar{q}^j P_{\mathrm{L}} \tilde{g}_a \tilde{q}^k_{\mathrm{R}}), \tag{3.1.3}$$

$$L_3 = \tfrac{\mathrm{i}}{2} g_s f_{abc} \bar{\tilde{g}}^a \gamma_\mu \tilde{g}^b A^c_\mu, \tag{3.1.4}$$

$$L_4 = \tfrac{1}{6} g_s^2 A^a_\mu A^\mu_a (\tilde{q}^*_{\mathrm{L}}\tilde{q}_{\mathrm{L}} + \tilde{q}^*_{\mathrm{R}}\tilde{q}_{\mathrm{R}}) + \tfrac{1}{2} g_s^2 d_{abc} A^a_\mu A^{\mu b}(\tilde{q}^{i*}_{\mathrm{L}} T^c_{ij} \tilde{q}^j_{\mathrm{L}} + \tilde{q}^{i*}_{\mathrm{R}} T^c_{ij} \tilde{q}^j_{\mathrm{R}}). \tag{3.1.5}$$

$q$ stands for quark, $\tilde{q}$ for the corresponding squark, $\tilde{g}$ for gluino, and $P_{\mathrm{L}}$ and $P_{\mathrm{R}}$ for left and right helicity projections, respectively. The mixing between the left- and right-handed stop quarks $\tilde{t}_{\mathrm{L}}$ and $\tilde{t}_{\mathrm{R}}$ can be very large due to the large mass of the top quark, and the lightest scalar top-quark mass eigenstate $\tilde{t}_1$ can be much lighter than the top quark and all the scalar partners of the light quarks. Therefore the left–right mixing for the SUSY partners of the top quark plays an important role. Here we only considered the SUSY QCD effect from the stop quark, because we assume that other scalar SUSY quarks are much heavier than the stop quark and hence decoupled. Furthermore, we introduce the phase angle $\phi_{\mathrm{A}}$ in the stop mixing matrix. Defining $\theta$ as mixing angle of stop quark, we have

$$\tilde{t}_{\mathrm{L}} = \mathrm{e}^{\frac{-\mathrm{i}\phi_{\mathrm{A}}}{2}}(\tilde{t}_1 \cos\theta + \tilde{t}_2 \sin\theta), \tag{3.1.6}$$

$$\tilde{t}_{\mathrm{R}} = \mathrm{e}^{\frac{\mathrm{i}\phi_{\mathrm{A}}}{2}}(-\tilde{t}_1 \sin\theta + \tilde{t}_2 \cos\theta), \tag{3.1.7}$$

where we suppose $m_{\tilde{t}_1} \le m_{\tilde{t}_2}$.

### 3.2 Analytical results of the MSSM QCD corrections

The one-loop SUSY QCD correction diagrams are shown in Fig. 1b. In the following we only present the amplitude expressions of the $s$-channel and the $t$-channel. The amplitude of the $u$-channel can be obtained from the $t$-channel expressions by the following variable exchanges: $t \leftrightarrow u$, $k_1 \leftrightarrow k_2$, $\epsilon^a_\mu(k_1) \leftrightarrow \epsilon^b_\nu(k_2)$ and $T^a \leftrightarrow T^b$. The one-loop diagrams can be divided into three groups: the self-energy diagrams of the gluon and the top quark shown in Fig. 1b.1; $gt\bar{t}$ and $ggg$ vertex correction diagrams shown in

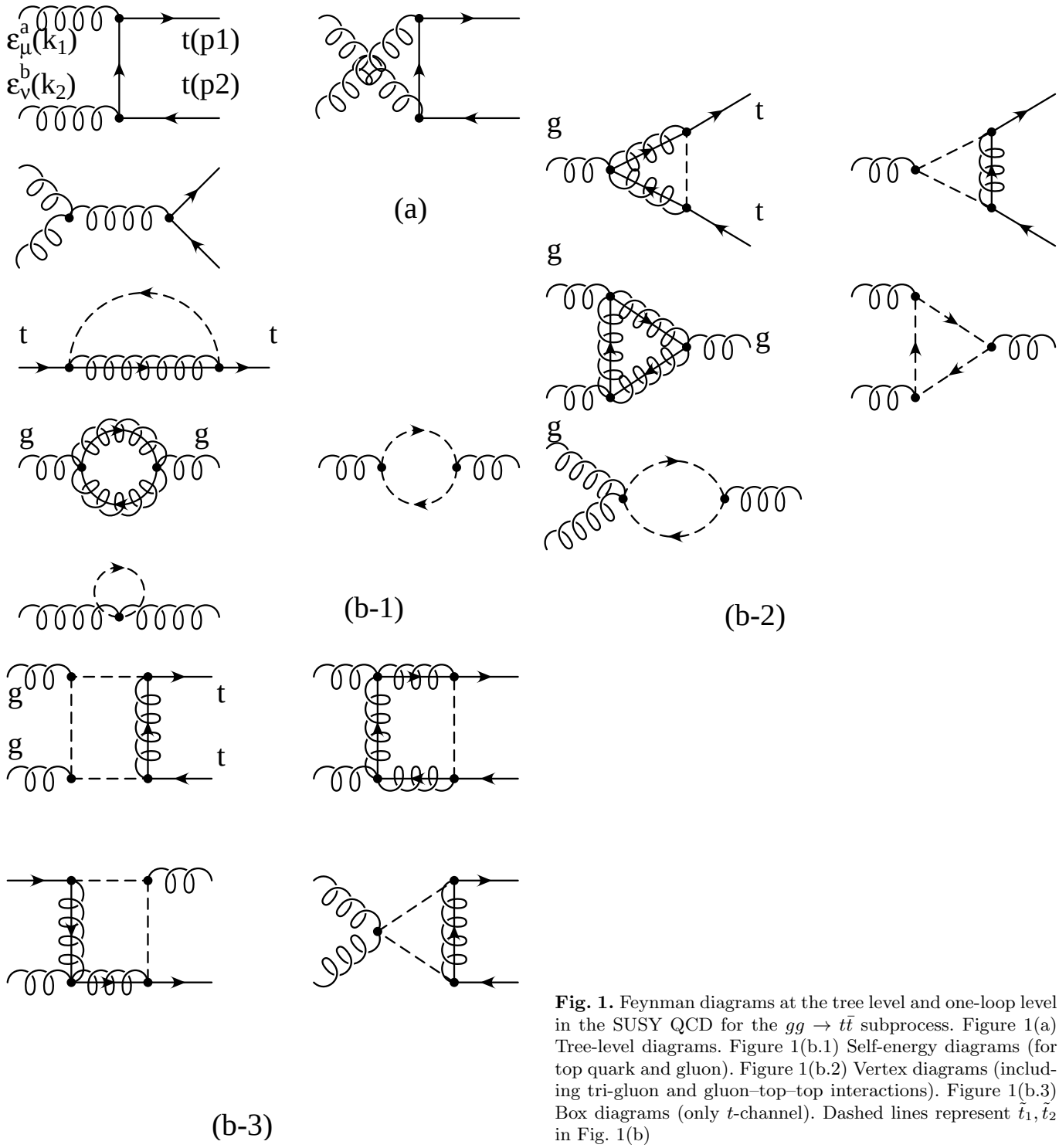


**Fig. 1.** Feynman diagrams at the tree level and one-loop level in the SUSY QCD for the $gg \to t\bar{t}$ subprocess. Figure 1(a) Tree-level diagrams. Figure 1(b.1) Self-energy diagrams (for top quark and gluon). Figure 1(b.2) Vertex diagrams (including tri-gluon and gluon–top–top interactions). Figure 1(b.3) Box diagrams (only $t$-channel). Dashed lines represent $\tilde{t}_1, \tilde{t}_2$ in Fig. 1(b)

Fig. 1b.2; and box diagrams shown in Fig. 1b.3. The ultraviolet divergence is controlled by dimensional regularization ($n = 4 - \epsilon$). The strong coupling-constants are renormalized by using the modified minimal subtraction ($\overline{\rm MS}$) scheme at charge-renormalization scale $\mu_{\rm R}$. This scheme violates SUSY explicitly, and the $q\tilde{q}\tilde{g}$ Yukawa coupling $\hat{g}_s$, which should be the same with the $qqg$ gauge coupling $g_s$ in supersymmetry, takes a finite shift at one-loop order. Therefore we take this shift to be between $\hat{g}_s$ and $g_s$ as shown in (3.2.1) into account in our calculation, so the physical amplitudes are independent of the renormalization scheme, and we subtract the contribution of the false, non-supersymmetric degrees of freedom (also called $\epsilon$ scalars) [12]:

$$\hat{g}_s = g_s \left[1 + \frac{\alpha_s}{4\pi}\left(\frac{2}{3}C_{\rm A} - \frac{1}{2}C_{\rm F}\right)\right], \qquad (3.2.1)$$

where $C_{\rm A}=3$ and $C_{\rm F}=4/3$ are the Casimir invariants of the SU(3) gauge group. The heavy particles (top quarks, gluino, stop quarks, etc.) are removed from the $\mu_{\rm R}$ evolution of $\alpha_s(\mu_{\rm R}^2)$; then they are decoupled smoothly when momenta are smaller than their masses [13]. We define masses of heavy particles as pole masses.

The renormalized amplitude corresponding to all SUSY QCD one-loop corrections (as shown in Fig. 1) can be split into the following components:

$$\delta M=\delta M_s+\delta M_v+\delta M_{\rm box}+\delta M_d, \tag{3.2.2}$$

where $\delta M_s$, $\delta M_v$, $\delta M_{\rm box}$ and $\delta M_d$ are the one-loop amplitudes corresponding to the self-energy, vertex, and box correction diagrams and the decoupling part, respectively. The $\delta M_d$ stems from the decoupling of the heavy flavors from the running strong coupling, and is given explicately by (see also [12,13]):

$$\begin{aligned}\delta M_d=M_0(\tfrac{\alpha_s(\mu)}{\pi})[&\tfrac{1}{24}\log(\tfrac{\mu_{\rm R}^2}{m_{\tilde t_1}^2})+\tfrac{1}{24}\log(\tfrac{\mu_{\rm R}^2}{m_{\tilde t_2}^2})\\&+\tfrac{1}{6}\log(\tfrac{\mu_{\rm R}^2}{m_t^2})+\tfrac{1}{2}\log(\tfrac{\mu_{\rm R}^2}{m_{\tilde g}^2})].\end{aligned} \tag{3.2.3}$$

### 3.3 Self-energy corrections to the amplitude

The amplitude of self-energy diagrams $\delta M_s$ (Fig. 1b.1) can be decomposed into $\delta M_s^g$ (gluon self-energy) and $\delta M_s^q$ (top-quark self-energy), i.e.

$$\begin{aligned}\delta M_s&=\delta M_s^g+\delta M_s^q\\&=\delta M_s^{g(s)}+\delta M_s^{g(t)}+\delta M_s^{g(u)}+\delta M_s^{q(t)}+\delta M_s^{q(u)}.\end{aligned} \tag{3.3.1}$$

The amplitudes $\delta M_s^{g(s)}$, $\delta M_s^{g(t)}$ and $\delta M_s^{g(u)}$ are for the $s$-, $t$- and $u$-channel, respectively. They can be expressed as:

$$\delta M_s^{g(s)}=\tfrac{1}{2}M_0^{(s)}[\Pi(k_1^2)+\Pi(k_2^2)+2\Pi(s)], \tag{3.3.2}$$

$$\delta M_s^{g(t)}=\tfrac{1}{2}M_0^{(t)}[\Pi(k_1^2)+\Pi(k_2^2)], \tag{3.3.3}$$

$$\delta M_s^{g(u)}=\tfrac{1}{2}M_0^{(u)}[\Pi(k_1^2)+\Pi(k_2^2)], \tag{3.3.4}$$

where $M_0$ is the tree-level amplitude defined in (2.4).

$$\begin{aligned}\Pi(k^2)=-\tfrac{\alpha_s}{4\pi}(&T_{\rm F}(\bar B_0+4\bar B_1+4\bar B_{21})[k,m_{\tilde t_1},m_{\tilde t_1}]\\&+T_{\rm F}(\bar B_0+4\bar B_1+4\bar B_{21})[k,m_{\tilde t_2},m_{\tilde t_2}]\\&-4C_{\rm A}(\bar B_1+\bar B_{21})[k,m_{\tilde g},m_{\tilde g}]-\tfrac{1}{3}C_{\rm A}).\end{aligned} \tag{3.3.5}$$

where $C_{\rm F}=4/3$, $T_{\rm F}=1/2$ and $C_{\rm A}=3$ are invariants in the SU(3) color group, and $B_i$ and $B_{ij}$ are Passarino–Veltman two-point functions [14,15]. The definitions of $\bar B_0$, $\bar B_1$ and $\bar B_{21}$ are listed in Appendix A. The amplitude $\delta M_s^{q(t)}$ is written as:

$$\begin{aligned}\delta M_s^{q(t)}=&\tfrac{-{\rm i}g_s^2T_{ik}^aT_{lj}^b}{(t-m_t^2)^2}\epsilon^{\mu,a}(k_1)\epsilon^{\nu,b}(k_2)\bar u_i(p_1)\gamma_\mu\\&(\not k_2-\not p_2+m_t)\left[\hat\Sigma_{kl}(k_2-p_2)\right]\\&\times(\not k_2-\not p_2+m_t)\gamma_\nu v_j(p_2).\end{aligned} \tag{3.3.6}$$

Here we define

$$\hat\Sigma_{kl}(p)=C_{\rm F}(H_{\rm L}\not pP_{\rm L}+H_{\rm R}\not pP_{\rm R}-H_{\rm L}^{\rm S}P_{\rm L}-H_{\rm R}^{\rm S}P_{\rm R})\delta_{kl}, \tag{3.3.7}$$

with

$$\begin{aligned}H_{\rm L}=&\tfrac{\hat g_s^2}{8\pi^2}x_1x_3B_1[p,m_{\tilde g},m_{\tilde t_1}]\\&+(m_{\tilde t_1}\to m_{\tilde t_2},x_i\to y_i)\\&+\tfrac{1}{2}(\delta Z_{\rm L}+\delta Z_{\rm L}^\dagger),\end{aligned} \tag{3.3.8}$$

$$\begin{aligned}H_{\rm R}=&\tfrac{\hat g_s^2}{8\pi^2}x_2x_4B_1[p,m_{\tilde g},m_{\tilde t_1}]\\&+(m_{\tilde t_1}\to m_{\tilde t_2},x_i\to y_i)\\&+\tfrac{1}{2}(\delta Z_{\rm R}+\delta Z_{\rm R}^\dagger),\end{aligned} \tag{3.3.9}$$

$$\begin{aligned}H_{\rm L}^{\rm S}=&\tfrac{\hat g_s^2}{8\pi^2}x_2x_3m_{\tilde g}B_0[p,m_{\tilde g},m_{\tilde t_1}]\\&+(m_{\tilde t_1}\to m_{\tilde t_2},x_i\to y_i)\\&+\tfrac{1}{2}m_t(\delta Z_{\rm L}+\delta Z_{\rm R}^\dagger)+\delta m_t,\end{aligned} \tag{3.3.10}$$

$$\begin{aligned}H_{\rm R}^{\rm S}=&\tfrac{\hat g_s^2}{8\pi^2}x_1x_4m_{\tilde g}B_0[p,m_{\tilde g},m_{\tilde t_1}]\\&+(m_{\tilde t_1}\to m_{\tilde t_2},x_i\to y_i)\\&+\tfrac{1}{2}m_t(\delta Z_{\rm R}+\delta Z_{\rm L}^\dagger)+\delta m_t,\end{aligned} \tag{3.3.11}$$

where we abbreviate $\phi=\phi_{\rm A}$, $x_1=\cos\theta{\rm e}^{-{\rm i}\phi}$, $x_2=\sin\theta{\rm e}^{{\rm i}\phi}$, $x_3=\cos\theta{\rm e}^{{\rm i}\phi}$, $x_4=\sin\theta{\rm e}^{-{\rm i}\phi}$, $y_1=\sin\theta{\rm e}^{-{\rm i}\phi}$, $y_2=-\cos\theta{\rm e}^{{\rm i}\phi}$, $y_3=\sin\theta{\rm e}^{{\rm i}\phi}$, $y_4=-\cos\theta{\rm e}^{-{\rm i}\phi}$, and $\theta$ is the mixing angle of stop quarks (see (3.1.6) and (3.1.7)).

The explicit expressions of the top-quark wave-function renormalization constants have the following forms:

$$\begin{aligned}\delta Z_{\rm L}=&-\tfrac{\hat g_s^2}{8\pi^2}(x_1x_3{\rm Re}[B_1]-\tfrac{m_{\tilde g}}{m_t}(x_1x_4-x_2x_3){\rm Re}[B_0]\\&+m_t^2(x_1x_3+x_2x_4){\rm Re}[B_1^{'}]\\&-m_tm_{\tilde g}(x_2x_3+x_1x_4){\rm Re}[B_0^{'}])[p,m_{\tilde g},m_{\tilde t_1}]|_{p^2=m_t^2},\end{aligned} \tag{3.3.12}$$

$$\begin{aligned}\delta Z_{\rm R}=&-\tfrac{\hat g_s^2}{8\pi^2}(x_2x_4{\rm Re}[B_1]+m_t^2(x_1x_3+x_2x_4){\rm Re}[B_1^{'}]\\&-m_tm_{\tilde g}(x_2x_3+x_1x_4){\rm Re}[B_0^{'}])[p,m_{\tilde g},m_{\tilde t_1}]|_{p^2=m_t^2},\end{aligned} \tag{3.3.13}$$

$$\begin{aligned}\delta m_t=&\tfrac{\hat g_s^2}{16\pi^2}((x_1x_3+x_2x_4)m_t{\rm Re}[B_1]\\&-(x_2x_3+x_1x_4)m_{\tilde g}{\rm Re}[B_0])[p,m_{\tilde g},m_{\tilde t_1}]|_{p^2=m_t^2}.\end{aligned} \tag{3.3.14}$$

We use the following abbreviations: $B_{i,ij}^{'}[p,m_1,m_2]=\partial B_{i,ij}[p,m_1,m_2]/\partial p^2$.

### 3.4 Vertex-corrections to the amplitude

The amplitudes for vertex diagrams can be expressed as:

$$\delta M_v^{(l)}=g_s\epsilon^{\mu,a}(k_1)\epsilon^{\nu,b}(k_2)\bar u_i(p_1)\Lambda^{(l)}v_j(p_2),\quad(l=s,t,u), \tag{3.4.1}$$

where

$$\begin{aligned}\Lambda^{(s)}=&-\tfrac{T_{ij}^c}{s}\left[\Lambda_{\mu\nu\rho}^{(3g)}(k_1,k_2)\right]\gamma_\rho\\&-\tfrac{f_{abc}}{s}[(k_1-k_2)_\rho g_{\mu\nu}+(2k_2+k_1)_\mu g_{\nu\rho}\\&-(2k_1+k_2)_\nu g_{\mu\rho}]\left[\Lambda_{\rho,(ij)}^c(p_1,p_2)\right]\end{aligned} \tag{3.4.2}$$

and

$$\Lambda^{(t)} = \frac{-\mathrm{i}}{t-m_t^2}\left\{T^b_{mj}\left[\Lambda^a_{\mu,(im)}(p_1,k_1-p_1)\right](\not{k}_2-\not{p}_2+m_t)\gamma_\nu + T^a_{im}\gamma_\mu(\not{k}_2-\not{p}_2+m_t)\left[\Lambda^b_{\nu,(mj)}(k_2-p_2,p_2)\right]\right\}. \tag{3.4.3}$$

The functions $\Lambda^{(3g)}_{\mu\nu\rho}$ and $\Lambda^a_{\mu,(ij)}$ are listed in Appendix B.

### 3.5 Box corrections to the amplitude

The box-diagram corrections in the $t$-channel (Fig. 1b.3) are given as follows:

$$\begin{aligned}\delta M^{(t)}_{\mathrm{box}} = {} & 2g_s^2\epsilon^{\mu,a}(k_1)\epsilon^{\nu,b}(k_2)\bar{u}_i(p_1)((T^cT^aT^bT^c)_{ij}F^{(t1)}_{\mu\nu} \\ & -\mathrm{i}f_{bcd}(T^cT^aT^d)_{ij}F^{(t2)}_{\mu\nu} \\ & -f_{acm}f_{bmd}(T^cT^d)_{ij}F^{(t3)}_{\mu\nu} \\ & -[T^c(T^aT^b+T^bT^a)T^c]_{ij}F^{(t4)}_{\mu\nu})v_j(p_2),\end{aligned} \tag{3.5.1}$$

where $f_{abc}$ is defined as $[T^a,T^b]=\mathrm{i}f_{abc}T^c$. The form factors $F^{(ti)}_{\mu\nu}$ ($i$ = 1–4) correspond to the kernel of the four Feynman diagrams in Fig. 1b.3 respectively, and are given explicitly in Appendix C.

### 3.6 Total cross section

Collecting all terms in (3.2.2), we can get the total cross section:

$$\begin{aligned}\sigma(\lambda_1,\lambda_2) &= \sigma_0(\lambda_1,\lambda_2)(1+\delta\sigma(\lambda_1,\lambda_2)) \\ &= \tfrac{1}{16\pi s^2}\int_{t^-}^{t^+}\mathrm{d}t\textstyle\sum_{\mathrm{spins}}[|M_0|^2+2\mathrm{Re}(M_0^\dagger\delta M)],\end{aligned} \tag{3.6.1}$$

where $t^\pm=(m_t^2-(1/2)s)\pm(1/2)s\beta_t$, $\beta_t=\sqrt{1-4m_t^2/s}$, and the spin sum is performed only over the final top-quark pair when we considered polarized gluons.

## 4 Numerical results

We write $\hat{\sigma}_0$ for the Born cross section and $\hat{\sigma}$ for the cross section including one-loop SUSY QCD corrections of subprocess $gg\to t\bar{t}$, and define its relative correction as $\hat{\delta}=(\hat{\sigma}-\hat{\sigma}_0)/\hat{\sigma}_0$. For polarized gluon fusions, $\hat{\sigma}_{++}$, $\hat{\sigma}_{--}$ and $\hat{\sigma}_{+-}$ are the cross sections with positive, negative and mixed polarization of the gluons, respectively. In order to inspect the CP-violating effects we introduce the CP-violation parameter for the subprocess defined by $\hat{\xi}_{\mathrm{CP}}=(\hat{\sigma}_{++}-\hat{\sigma}_{--})/(\hat{\sigma}_{++}+\hat{\sigma}_{--})$. The possible SUSY QCD effects in $gg\to t\bar{t}$ should be observed in $pp$ colliders. By analogy we can also define the relative correction and the CP-violating parameter for the process $pp\to gg\to t\bar{t}x$ as $\delta=(\sigma-\sigma_0)/\sigma_0$ and $\xi_{\mathrm{CP}}=(\sigma_{++}-\sigma_{--})/(\sigma_{++}+\sigma_{--})$, respectively. The SUSY QCD contribution to the process $p(P_1,x)p(P_2,y)\to gg\to t\bar{t}X$ ($x$ and $y$ are polarizations of protons) can be obtained by convoluting the subprocess with gluon distribution functions;

$$\sigma(s)=\int\mathrm{d}x_1\mathrm{d}x_2G(x_1,Q)G(x_2,Q)\hat{\sigma}(\hat{s},\alpha_s(\mu)), \tag{4.1}$$

with $k_1=x_1P_1$, $k_2=x_2P_2$ and $\tau=x_1x_2=\hat{s}/s$. $G(x_i,Q)$ ($i=1,2$) are gluon distribution functions of protons. We take $Q=\mu_{\mathrm{R}}=2m_t$.

In order to get results of top-quark pair production from polarized $pp$ collisions, we need to consider the polarized gluon distributions in protons. The cross sections of polarized $pp\to gg\to t\bar{t}X$ can be written as

$$\begin{aligned}\sigma(x,y) = {} & \Sigma_{\lambda_1,\lambda_2=\pm}\int\mathrm{d}x_1\mathrm{d}x_2G^{x\lambda_1}(x_1,Q) \\ & \times G^{y\lambda_2}(x_2,Q)\hat{\sigma}_{\lambda_1,\lambda_2}(\hat{s},\alpha_s(\mu)),\end{aligned} \tag{4.2}$$

where $x$ and $y$ are the polarizations of incoming protons, and $\lambda_1$ and $\lambda_2$ are the polarizations of gluons inside protons. $G^{x\lambda_1}(x,Q)$, $G^{y\lambda_2}(x,Q)=G^{\pm}(x,Q)$ for equal (+) and opposite (−) polarizations, where $G^+(x,Q)$ and $G^-(x,Q)$ are polarized gluon distribution functions in the proton.

We used the unpolarized proton structure functions of Glück et al. [9] in our numerical calculations. For the polarized proton structure functions, we use the evolution equations of Glück et al. [10] with input parameters from the paper of Stratmann et al. [11] (next-to-leading order). Since the structure functions belong to the least certain inputs of our calculation, we checked the result against another set, i.e. the polarized structure functions $G^{\pm}(x,Q)$ of Brodsky et al. [8] (using leading order only). This tests the stability of our results against the particular form of the input structure functions. The two different sets of input are compared in Fig. 2, which gives the relative SUSY QCD correction ($\delta$) and $\xi_{\mathrm{CP}}$ versus c.m. energy $\sqrt{s}$ for the process $pp\to gg\to t\bar{t}X$. Though the SUSY QCD corrections from the two sets of structure functions are not very different for $\delta$, there is some noticeable change for $\xi_{\mathrm{CP}}$. Because $\xi_{\mathrm{CP}}$ depends strongly on the c.m. energy of the subprocess $gg\to t\bar{t}$ (shown in Fig. 3b), a small modification of the structure functions may lead to a large change of $\xi_{\mathrm{CP}}$. Thus we can infer that the NLO-QCD calculation is required and the precise numerical prediction does depend on the reliability of the structure functions.

The SUSY QCD relative corrections are about 2–4% and decrease with increasing c.m. energy (see Fig. 2). These correction effects are within reach of future precision experiments and provide a possible discrimination of the SM and the MSSM effects. From Fig. 2c we can see that the CP-violation parameter $\xi_{\mathrm{CP}}$ can be $10^{-3}$. Therefore, CP violation in this process stemming from the SUSY QCD can in principle be tested in future precision experiments. That would help us to learn more about the sources of CP violation.

In order to explore the effects of the SUSY QCD correction for future arrangements of optimal experimental conditions, we also investigate the subprocess $gg\to t\bar{t}$.

The relative SUSY QCD correction and CP-violating parameter versus c.m. energy ($\sqrt{\hat{s}}$) for different polarization gluons are plotted in Fig. 3a–c with $m_{\tilde{g}}=200\,\mathrm{GeV}$, $m_{\tilde{t}_1}=250\,\mathrm{GeV}$, $m_{\tilde{t}_2}=450\,\mathrm{GeV}$, and $\theta=\phi=45°$. In Fig. 3a, $\hat{\delta}_{++}$ and $\hat{\delta}_{--}$ are shown by a solid line and a dashed line, respectively. $\hat{\xi}_{\mathrm{CP}}$ as a function of c.m. energy is depicted in Fig. 3b, and $\hat{\delta}_{+-}$ as a function of $\sqrt{\hat{s}}$ is

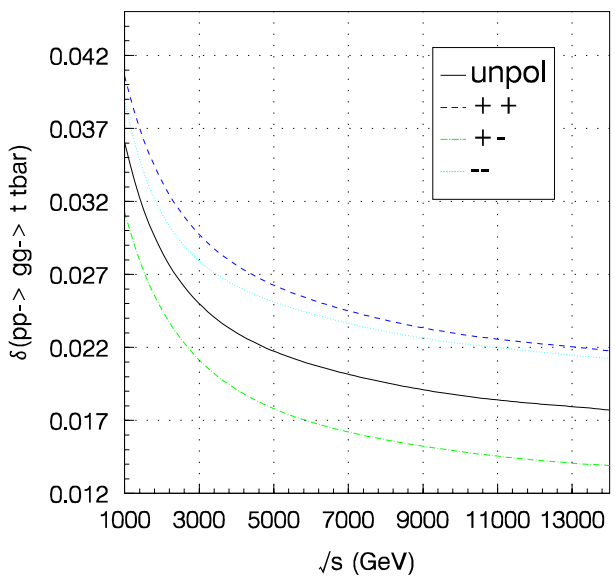


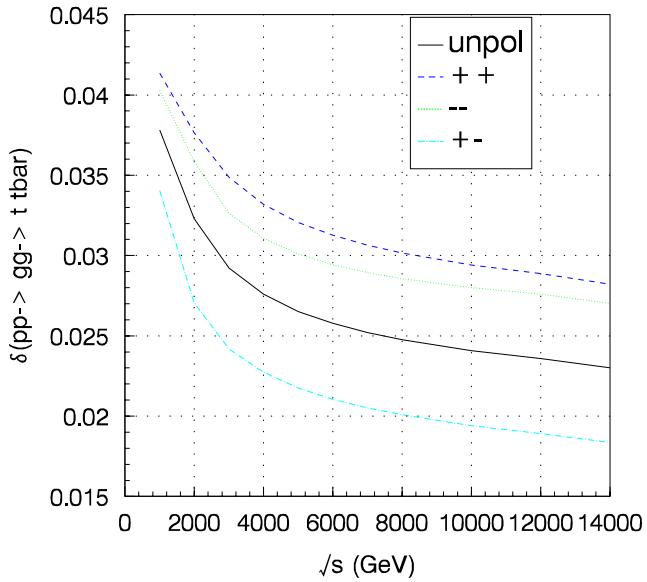


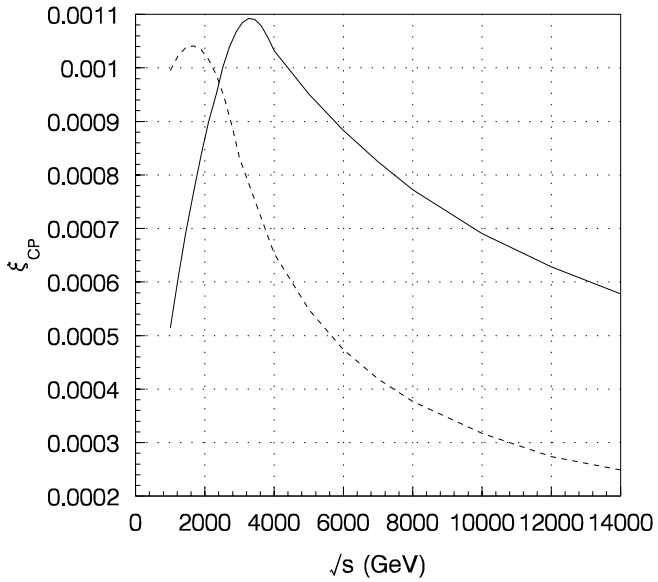


**Fig. 2. a** Relative corrections to polarized and unpolarized cross sections of the $t\bar{t}$ production process in $pp$ colliders as a function of $\sqrt{s}$ with input structure functions of Brodsky et al. [8] (LO). **b** Relative corrections to polarized and unpolarized cross sections of the $t\bar{t}$ production process in $pp$ colliders as a function of $\sqrt{s}$ with input structure functions of Glück et al. [9–11] (NLO). In both **a** and **b**, the solid line is for the MSSM QCD correction with unpolarized protons, the dashed line is for the MSSM QCD correction with proton(+) proton(+) polarization, the dotted line is for the MSSM QCD correction with proton(−) proton(−) polarization, and the dot-dashed line is for the MSSM QCD correction with proton(+) proton(−) polarization. **c** The CP-violating parameter $\xi_{\rm CP}$ as a function of $\sqrt{s}$. The solid line is for input structure functions of Glück et al. (NLO), the dashed line is for input structure functions of Brodsky et al. (LO) $m_{\tilde{g}} = 200\,\text{GeV}$, $m_{\tilde{t}_1} = 250\,\text{GeV}$, $m_{\tilde{t}_2} = 450\,\text{GeV}$ and $\theta = \phi = 45^\circ$

plotted in Fig. 3c. Each curve in Fig. 3a has an obvious peak near the position of the threshold of top pair production. That large enhancement is the combined effect of the threshold, when $\sqrt{\hat{s}}$ is just larger than $2m_t = 350\,\text{GeV}$, and the resonance when $\sqrt{\hat{s}} \sim 2m_{\tilde{g}} = 400\,\text{GeV}$. The small spikes around the position of $\sqrt{\hat{s}} = 900\,\text{GeV}$, where $\sqrt{\hat{s}} \sim 2m_{\tilde{t}_2} = 900\,\text{GeV}$, also shows the resonance effect. Although Fig. 3a shows that $\hat{\delta}_{++}$ and $\hat{\delta}_{--}$ approach equal values when the c.m. energy is far beyond its threshold value $2m_t$, the quantitative difference between $\hat{\delta}_{+-}$ and $\hat{\delta}_{++}$ still exists in the whole energy range plotted in these figures. Figure 3b also shows that $\hat{\xi}_{\rm CP}$ will be zero if the c.m. energy is below the threshold of SUSY particles in the loop (i.e. $\sqrt{\hat{s}} \leq 2m_{\tilde{g}} = 400\,\text{GeV}$ in Fig. 3b. This is reasonable because only beyond this point we can have absorptive terms which give contributions to $\hat{\xi}_{\rm CP}$. $\hat{\xi}_{\rm CP}$ has an obvious resonance effect in the regions around $\sqrt{\hat{s}} \sim 2m_{\tilde{g}} = 400\,\text{GeV}$ and $\sqrt{\hat{s}} \sim 2m_{\tilde{t}_i}$ $(i = 1, 2) = 500\,\text{GeV}$, $900\,\text{GeV}$. We also find that the two stop quarks give opposite contributions to $\hat{\xi}_{\rm CP}$, and when their masses are degenerate $\hat{\xi}_{\rm CP}$ will vanish. When the c.m. energy $\sqrt{\hat{s}}$ is larger than 1 TeV, $\hat{\xi}_{\rm CP}$ will be near zero, because the contributions from the two stop quarks will cancel each other. Therefore a quantitative strong change of $\hat{\xi}_{\rm CP}$ as a function of c.m. energy can be an indication for the signals of stop quarks and gluino.

$\hat{\sigma}(\pm, \pm)$ and $\hat{\xi}_{\rm CP}$ as functions of $m_{\tilde{g}}$ are shown in Fig. 4a and b, respectively. In Fig. 4 we take $\sqrt{\hat{s}} = 500\,\text{GeV}$, $m_{\tilde{t}_1} = 100\,\text{GeV}$, $m_{\tilde{t}_2} = 450\,\text{GeV}$, and $\theta = \phi = 45^\circ$. We can see from Fig. 4b that $\hat{\xi}_{\rm CP}$ changes its sign when $m_{\tilde{g}}$ is near $m_t = 175\,\text{GeV}$. The curves in Fig. 4a, b

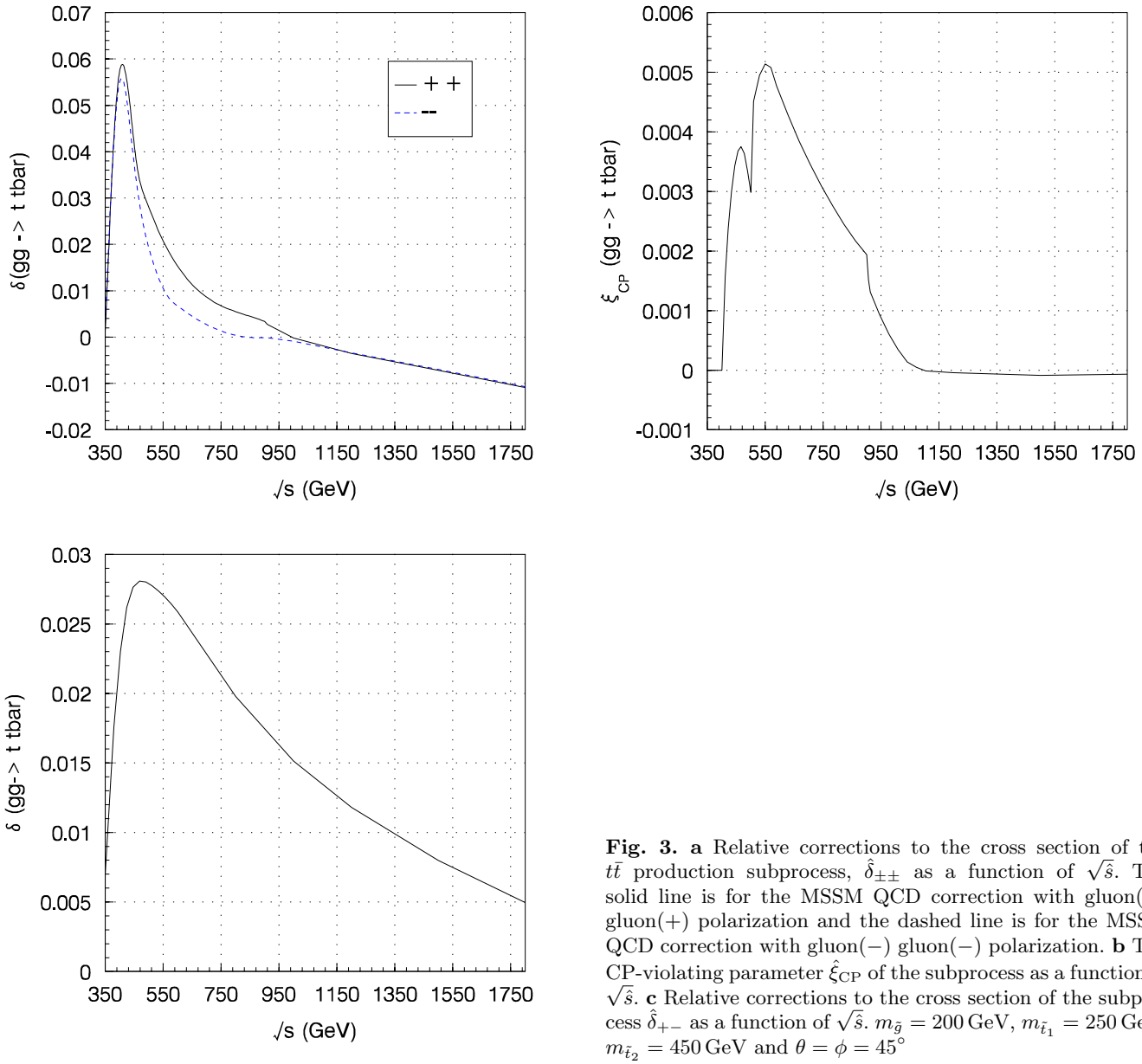


**Fig. 3.** **a** Relative corrections to the cross section of the $t\bar{t}$ production subprocess, $\hat{\delta}_{\pm\pm}$ as a function of $\sqrt{\hat{s}}$. The solid line is for the MSSM QCD correction with gluon(+) gluon(+) polarization and the dashed line is for the MSSM QCD correction with gluon(−) gluon(−) polarization. **b** The CP-violating parameter $\hat{\xi}_{\rm CP}$ of the subprocess as a function of $\sqrt{\hat{s}}$. **c** Relative corrections to the cross section of the subprocess $\hat{\delta}_{+-}$ as a function of $\sqrt{\hat{s}}$. $m_{\tilde{g}} = 200\,\text{GeV}$, $m_{\tilde{t}_1} = 250\,\text{GeV}$, $m_{\tilde{t}_2} = 450\,\text{GeV}$ and $\theta = \phi = 45^\circ$

again show the resonance effect when $\sqrt{\hat{s}} \sim 2m_{\tilde{g}} = 500\,\text{GeV}$. Note that for each line there is a steep change of the value of $\hat{\sigma}(\pm,\pm)$ or $\hat{\xi}_{\rm CP}$ around the position of $m_{\tilde{g}} = 250\,\text{GeV}$.

Dependences of the relative correction $\hat{\delta}_{\pm\pm}$ and $\hat{\xi}_{\rm CP}$ for the subprocess $gg \to t\bar{t}$ on $m_{\tilde{t}_1}$ are plotted in Fig. 5a, b. $\hat{\delta}_{\pm\pm}$ and $\hat{\xi}_{\rm CP}$ as functions of $m_{\tilde{t}_2}$ are shown in Fig. 6a and b, respectively. In all parts of Figs. 5 and 6, we take the common parameter set with $\sqrt{\hat{s}} = 500\,\text{GeV}$, $m_{\tilde{g}} = 200\,\text{GeV}$ and $\theta = \phi = 45^\circ$. In Fig. 5 we set $m_{\tilde{t}_2} = 450\,\text{GeV}$, whereas $m_{\tilde{t}_1} = 100\,\text{GeV}$ in Fig. 6. We find that $\hat{\xi}_{\rm CP}$ in fact increases with mass splitting of stop quarks (i.e. $m_{\tilde{t}_2} - m_{\tilde{t}_1}$), and when $m_{\tilde{t}_1} = m_{\tilde{t}_2}$, $\hat{\xi}_{\rm CP}$ is equal to zero. The resonance effect of stop quarks, when $\sqrt{\hat{s}} \sim 2m_{\tilde{t}_i}$ $(i = 1, 2)$, is superimposed on the curves in Fig. 5a, b and Fig. 6a, b around the positions of $m_{\tilde{t}_1} = 250\,\text{GeV}$ in Fig. 5a, b and $m_{\tilde{t}_2} = 250\,\text{GeV}$ in Fig. 6a, b. Around those points the relatively sharp changes of the values of $\hat{\xi}_{\rm CP}$ and the relative corrections are shown in these figures.

Finally, the dependence of $\hat{\delta}_{\pm\pm}$ and $\hat{\xi}_{\rm CP}$ on the phase $\phi$ is shown in Fig. 7a, b. In Fig. 7, we take $\sqrt{\hat{s}} = 500\,\text{GeV}$, $m_{\tilde{g}} = 200\,\text{GeV}$, $\theta = 45^\circ$ and $m_{\tilde{t}_1} = 150\,\text{GeV}$. We find that $\hat{\xi}_{\rm CP}$ is directly proportional to $\sin(2\phi)$ and reaches its maximum value when $\phi = \pi/4$.

## 5 Conclusion

In this work we have studied the one-loop supersymmetric QCD corrections to the subprocess $gg \to t\bar{t}$ and the process $pp \to gg \to t\bar{t}X$. The calculations show that the

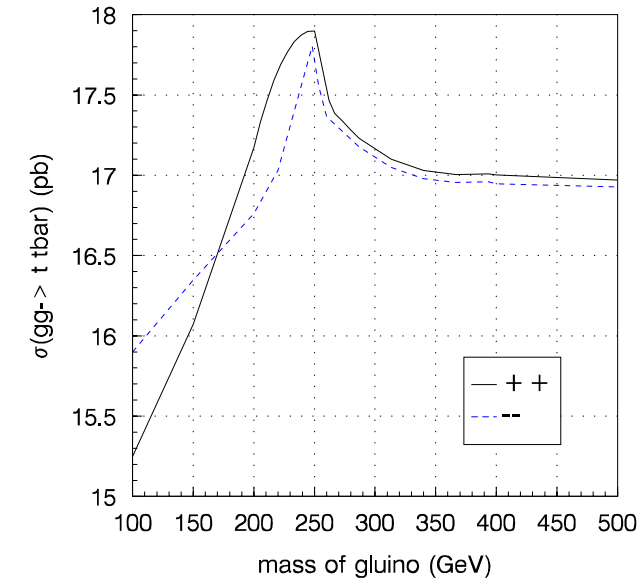


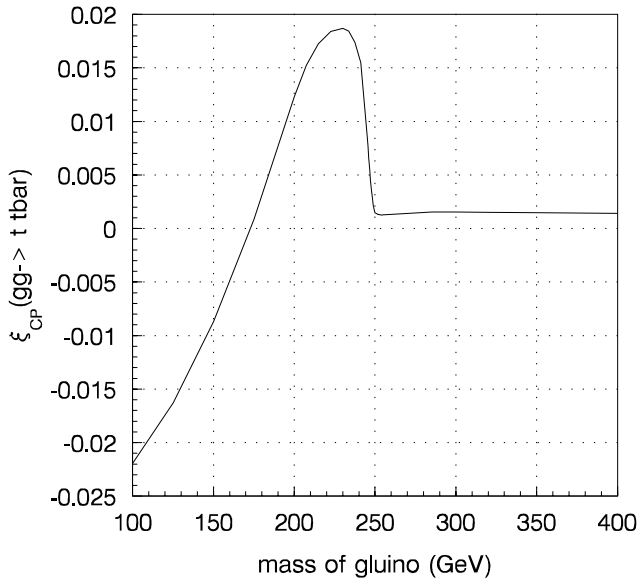


**Fig. 4. a** Cross section of the $t\bar{t}$ production subprocess via $gg$ fusion, $\hat{\sigma}_{\pm\pm}$ as a function of $m_{\tilde{g}}$. The solid line is for the MSSM QCD correction with gluon(+) gluon(+) polarization and the dashed line is for the MSSM QCD correction with gluon(−) gluon(−) polarization. **b** The CP-violating parameter $\hat{\xi}_{\rm CP}$ of the subprocess as a function of $m_{\tilde{g}}$. $m_{\tilde{t}_1} = 100\,{\rm GeV}$, $m_{\tilde{t}_2} = 450\,{\rm GeV}$, $\sqrt{\hat{s}} = 500\,{\rm GeV}$ and $\theta = \phi = 45^\circ$

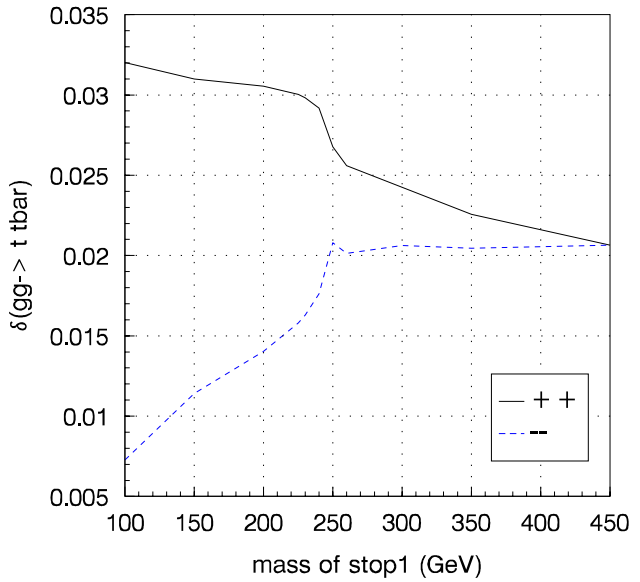


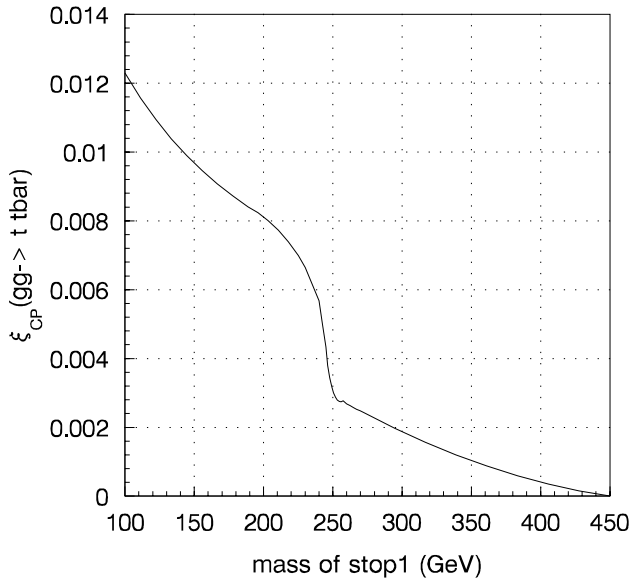


**Fig. 5. a** Relative corrections to the cross section of the $t\bar{t}$ production subprocess via $gg$ fusion, $\hat{\delta}_{\pm\pm}$ as a function of $m_{\tilde{t}_1}$. The solid line is for the MSSM QCD correction with gluon(+) gluon(+) polarization and the dashed line is for the MSSM QCD correction with gluon(−) gluon(−) polarization. **b** The CP-violating parameter $\hat{\xi}_{\rm CP}$ of the subprocess as a function of $m_{\tilde{t}_1}$. $m_{\tilde{g}} = 200\,{\rm GeV}$, $m_{\tilde{t}_2} = 450\,{\rm GeV}$, $\sqrt{\hat{s}} = 500\,{\rm GeV}$ and $\theta = \phi = 45^\circ$

SUSY QCD effects are significant. The absolute values of the corrections are about 2–4%, so they may be observable in future precision experiments. Furthermore, we find $\xi_{\rm CP}$ depends strongly on the masses of SUSY particles and can reach $10^{-3}$ when we take plausible SUSY parameters.

The results show that there is an obvious difference between the corrections for the protons polarized with parallel spin and those with anti-parallel spin. Hence there is a possibility to study spin dependence in the frame of the MSSM QCD.

We also presented and discussed the results of the subprocess $gg \to t\bar{t}$. We find that, when the c.m. energy passes through the value $2m_{\tilde{g}}$ or $2m_{\tilde{t}_i}$ $(i = 1, 2)$, the value of the CP-violating parameter $\hat{\xi}_{\rm CP}$ changes considerably. If the c.m. energy is less than both $2m_{\tilde{g}}$ and $2m_{\tilde{t}_i} (i = 1, 2)$, $\hat{\xi}_{\rm CP}$ will be zero. If in future experiments a sharp change in $\hat{\xi}_{\rm CP}$ is found with $\sqrt{\hat{s}}$ running from low c.m. energy to high c.m. energy, it would be interpreted as a signal of

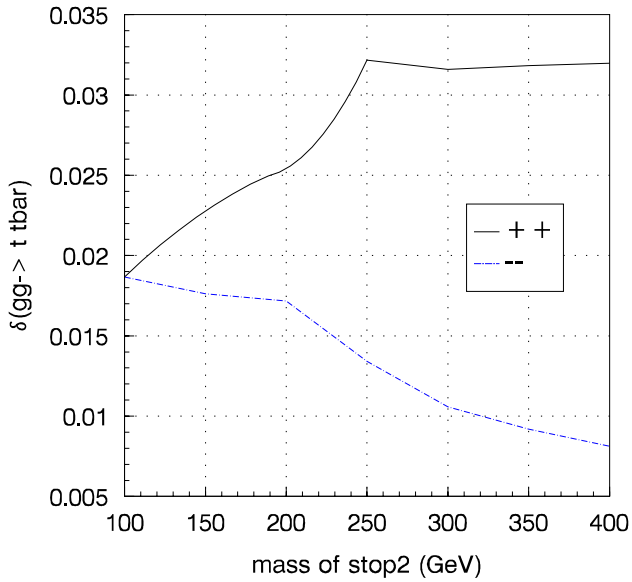


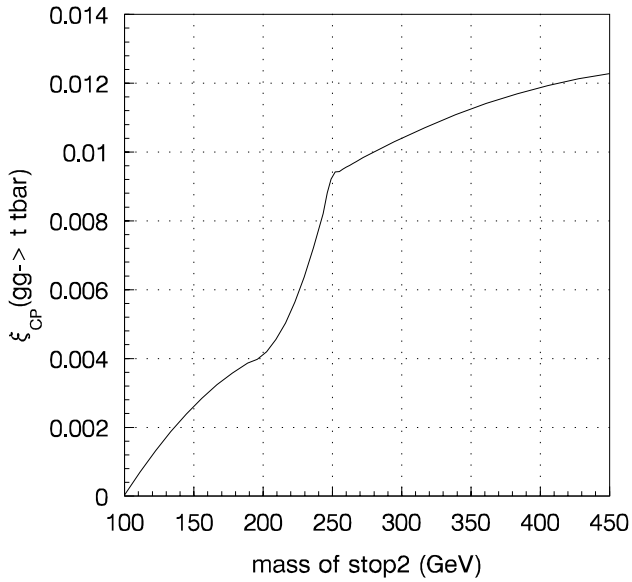


**Fig. 6. a** Relative corrections to the cross section of the $t\bar{t}$ production subprocess via $gg$ fusion, $\hat{\delta}_{\pm\pm}$ as a function of $m_{\tilde{t}_2}$. The solid line is for the MSSM QCD correction with gluon(+) gluon(+) polarization and the dashed line is for the MSSM QCD correction with gluon(−) gluon(−) polarization. **b** The CP-violating parameter $\hat{\xi}_{\rm CP}$ of the subprocess as a function of $m_{\tilde{t}_2}$. $m_{\tilde{g}} = 200\,\text{GeV}$, $m_{\tilde{t}_1} = 100\,\text{GeV}$ and $\sqrt{\hat{s}} = 500\,\text{GeV}$ and $\theta = \phi = 45°$

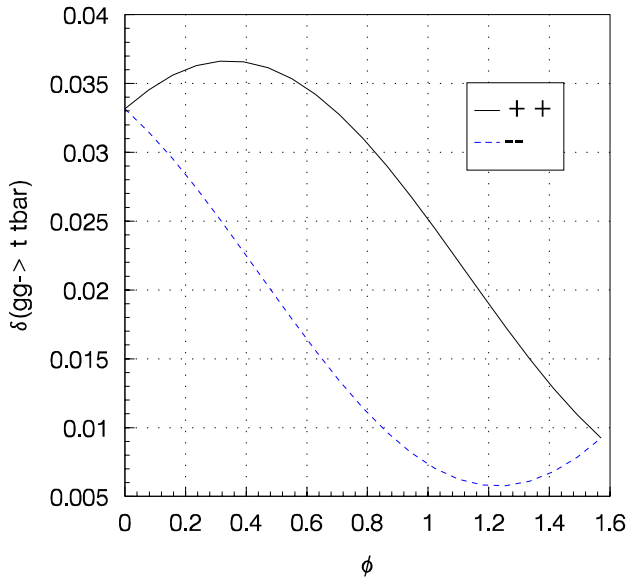


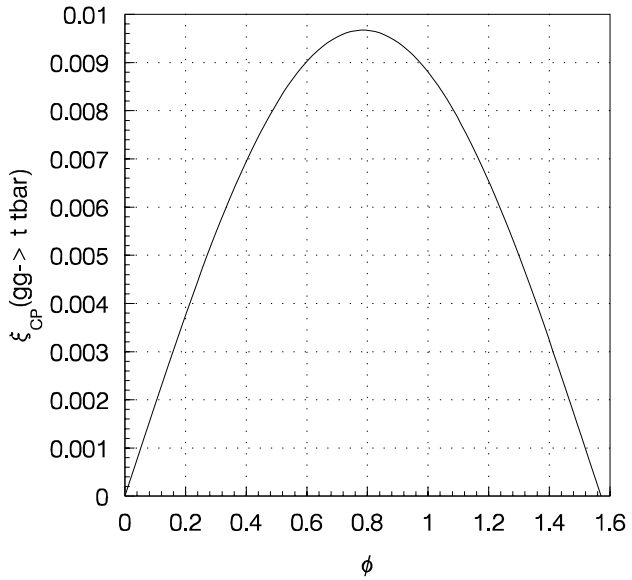


**Fig. 7. a** Relative corrections to the cross section of the $t\bar{t}$ production subprocess via $gg$ fusion, $\hat{\delta}_{\pm\pm}$ as a function of $\phi$. The solid line is for the MSSM QCD correction with gluon(+) gluon(+) polarization and the dashed line is for the MSSM QCD correction with gluon(−) gluon(−) polarization. **b** The CP-violating parameter $\hat{\xi}_{\rm CP}$ of the subprocess as a function of $\phi$. $m_{\tilde{g}} = 200\,\text{GeV}$,$m_{\tilde{t}_1} = 150\,\text{GeV}$, $m_{\tilde{t}_2} = 450\,\text{GeV}$,$\sqrt{\hat{s}} = 500\,\text{GeV}$ and $\theta = 45°$

SUSY particles. Furthermore, because the CP-violating parameter $\hat{\xi}_{\rm CP}$ is sensitive to the mass of the gluino (as shown in Fig. 4b) and the mass splitting of stop quarks $m_{\tilde{t}_2} - m_{\tilde{t}_1}$ (as shown in Figs. 5 and 6), we can also get information on SUSY particles from precise measurements of $\hat{\xi}_{\rm CP}$.

*Acknowledgements.* The authors would like to thank Prof. A. Bartl for useful discussions and comments. One of the authors, Yu Zeng-Hui, would like to thank Prof. H. Stremnitzer for his help.

## Appendix

### A. Loop integrals

We adopt the definitions of two-, three- and four-point one-loop Passarino–Veltman integral functions of [14,15].

1. The two-point integrals are:

$$\{B_0; B_\mu; B_{\mu\nu}\}(p, m_1, m_2) = \frac{(2\pi\mu)^{4-n}}{\mathrm{i}\pi^2}\int \mathrm{d}^n q \times \frac{\{1; q_\mu; q_\mu q_\nu\}}{[q^2 - m_1^2][(q+p)^2 - m_2^2]}, \tag{A.1}$$

The function $B_\mu$ is proportional to $p_\mu$:

$$B_\mu(p, m_1, m_2) = p_\mu B_1(p, m_1, m_2). \tag{A.2}$$

Similarly we define:

$$B_{\mu\nu} = p_\mu p_\nu B_{21} + g_{\mu\nu} B_{22}. \tag{A.3}$$

We define $\bar{B}_0 = B_0 - \Delta$, $\bar{B}_1 = B_1 + (1/2)\Delta$ and $\bar{B}_{21} = B_{21} - (1/3)\Delta$, with $\Delta = 2/\epsilon - \gamma + \log(4\pi)$, $\epsilon = 4 - n$. $\mu$ is the scale parameter.

2. The three-point integrals are:

$$\{C_0; C_\mu; C_{\mu\nu}; C_{\mu\nu\rho}\}(p, k, m_1, m_2, m_3) = -\frac{(2\pi\mu)^{4-n}}{\mathrm{i}\pi^2} \times \int \mathrm{d}^n q \frac{\{1; q_\mu; q_\mu q_\nu; q_\mu q_\nu q_\rho\}}{[q^2 - m_1^2][(q+p)^2 - m_2^2][(q+p+k)^2 - m_3^2]}. \tag{A.4}$$

We define form factors as follows:

$$\begin{aligned}
C_\mu &= p_\mu C_{11} + k_\mu C_{12},\\
C_{\mu\nu} &= p_\mu p_\nu C_{21} + k_\mu k_\nu C_{22} + (p_\mu k_\nu + k_\mu p_\mu) C_{23}\\
&\quad + g_{\mu\nu} C_{24},\\
C_{\mu\nu\rho} &= p_\mu p_\nu p_\rho C_{31} + k_\mu k_\nu k_\rho C_{32}\\
&\quad + (k_\mu p_\nu p_\rho + p_\mu k_\nu p_\rho + p_\mu p_\nu k_\rho) C_{33}\\
&\quad + (k_\mu k_\nu p_\rho + p_\mu k_\nu k_\rho + k_\mu p_\nu k_\rho) C_{34}\\
&\quad \times + (p_\mu g_{\nu\rho} + p_\nu g_{\mu\rho} + p_\rho g_{\mu\nu}) C_{35}\\
&\quad + (k_\mu g_{\nu\rho} + k_\nu g_{\mu\rho} + k_\rho g_{\mu\nu}) C_{36}.
\end{aligned} \tag{A.5}$$

3. The four-point integrals are:

$$\{D_0; D_\mu; D_{\mu\nu}; D_{\mu\nu\rho}; D_{\mu\nu\rho\alpha}\}(p, k, l, m_1, m_2, m_3, m_4) = \frac{(2\pi\mu)^{4-n}}{\mathrm{i}\pi^2}\int \mathrm{d}^n q \{1; q_\mu; q_\mu q_\nu; q_\mu q_\nu q_\rho; q_\mu q_\nu q_\rho q_\alpha\} \times \left\{[q^2 - m_1^2][(q+p)^2 - m_2^2] \times [(q+p+k)^2 - m_3^2][(q+p+k+l)^2 - m_4^2]\right\} \tag{A.6}$$

Again we define form factors of $D$ functions:

$$\begin{aligned}
D_\mu &= p_\mu D_{11} + k_\mu D_{12} + l_\mu D_{13},\\
D_{\mu\nu} &= p_\mu p_\nu D_{21} + k_\mu k_\nu D_{22} + l_\mu l_\nu D_{23} + \{pk\}_{\mu\nu} D_{24}\\
&\quad + \{pl\}_{\mu\nu} D_{25} + \{kl\}_{\mu\nu} D_{26} + g_{\mu\nu} D_{27},\\
D_{\mu\nu\rho} &= p_\mu p_{nu} p_\rho D_{31} + k_\mu k_{nu} k_\rho D_{32} + l_\mu l_{nu} l_\rho D_{33}\\
&\quad + \{kpp\}_{\mu\nu\rho} D_{34} + \{lpp\}_{\mu\nu\rho} D_{35} + \{pkk\}_{\mu\nu\rho} D_{36}\\
&\quad + \{pll\}_{\mu\nu\rho} D_{37} + \{lkk\}_{\mu\nu\rho} D_{38} + \{kll\}_{\mu\nu\rho} D_{39}\\
&\quad + \{pkl\}_{\mu\nu\rho} D_{310} + \{pg\}_{\mu\nu\rho} D_{311} + \{kg\}_{\mu\nu\rho} D_{312}\\
&\quad + \{lg\}_{\mu\nu\rho} D_{313},
\end{aligned} \tag{A.7}$$

where

$$\begin{aligned}
\{pk\}_{\mu\nu} &= p_\mu k_\nu + k_\mu p_\nu,\\
\{pkl\}_{\mu\nu\rho} &= p_\mu k_\nu l_\rho + l_\mu p_\nu k_\rho + k_\mu l_\nu p_\rho,\\
\{pg\}_{\mu\nu\rho} &= p_\mu g_{\nu\rho} + p_\nu g_{\mu\rho} + p_\rho g_{\mu\nu}.
\end{aligned} \tag{A.8}$$

The numerical calculation of the vector and tensor loop integral functions can be traced back to the four scalar loop integrals $A_0$, $B_0$, $C_0$ and $D_0$ in [14,15] and the references therein.

### B. Vertex corrections

The 3-gluon-vertex can be written as ($a$, $b$ and $c$ are the color indices of the external gluons):

$$\Lambda^{(3g)}_{\mu\nu\rho}(k_1, k_2) = \frac{\mathrm{i}g_s^3}{16\pi^2}\left\{\mathrm{Tr}(T^b T^c T^a)\left[\Lambda^{(1)}_{\mu\nu\rho}(k_1, k_2)\right] + \mathrm{i}f^{cmn} f^{anl} f^{blm}\left[\Lambda^{(2)}_{\mu\nu\rho}(k_1, k_2)\right]\right\}; \tag{B.1}$$

the vertex functions $\Lambda^{(1)}_{\mu\nu\rho}$, $\Lambda^{(2)}_{\mu\nu\rho}$ are expressed as follows:

$$\begin{aligned}
\Lambda^{(a)}_{\mu\nu\rho}(k_1, k_2) &= f_1^{(a)} g_{\mu\rho} k_{1\nu} + f_2^{(a)} g_{\mu\nu} k_{1\rho}\\
&\quad + f_3^{(a)} g_{\nu\rho} k_{2\mu} + f_4^{(a)} g_{\mu\nu} k_{2\rho}\\
&\quad + f_5^{(a)} k_{1\nu} k_{1\rho} k_{2\mu} + f_6^{(a)} k_{1\nu} k_{2\rho} k_{2\mu}\\
&\quad + (m_{\tilde{t}_1} \to m_{\tilde{t}_2}, x_i \to y_i),
\end{aligned} \tag{B.2}$$

where $a = 1, 2$, and the $f_i^{(1)}, f_i^{(2)}$ are given in terms of the Passarino–Veltman functions with internal stop lines $C_{ij}^{(1)} (= C_{ij}[-k_1, -k_2, m_{\tilde{t}_1}, m_{\tilde{t}_1}, m_{\tilde{t}_1}])$ and internal gluino lines $C_{ij}^{(2)} (= C_{ij}[-k_1, -k_2, m_{\tilde{g}}, m_{\tilde{g}}, m_{\tilde{g}}])$. For simplicity, we abbreviate the definite part of $C$ integral functions (using the definitions of [14,15]) as follows: $\bar{C}_{24}^{(a)} = C_{24}^{(a)} - \frac{1}{4}\Delta$, $\bar{C}_{35}^{(a)} = C_{35}^{(a)} + \frac{1}{6}\Delta$, $\bar{C}_{36}^{(a)} = C_{35}^{(a)} + \frac{1}{12}\Delta$ ($a = 1, 2$):

$$\begin{aligned}
f_1^{(1)} &= -8\bar{C}_{24}^{(1)} - 8\bar{C}_{35}^{(1)},\\
f_2^{(1)} &= -4\bar{C}_{24}^{(1)} - 8\bar{C}_{35}^{(1)},\\
f_3^{(1)} &= -8\bar{C}_{36}^{(1)},\\
f_4^{(1)} &= -4\bar{C}_{24}^{(1)} - 8\bar{C}_{36}^{(1)},\\
f_5^{(1)} &= 4C_{12}^{(1)} + 12C_{23}^{(1)} + 8C_{33}^{(1)},\\
f_6^{(1)} &= 4C_{12}^{(1)} + 8C_{22}^{(1)} + 4C_{23}^{(1)} + 8C_{34}^{(1)},
\end{aligned} \tag{B.3}$$

and

$$\begin{aligned}
f_1^{(2)} &= -8m_{\tilde{g}}^2 C_0^{(2)} - 4m_{\tilde{g}}^2 C_{11}^{(2)} - 16\bar{C}_{24}^{(2)}\\
&\quad + 12\epsilon C_{24}^{(2)} - 8\bar{C}_{35}^{(2)} + 6\epsilon C_{35}^{(2)}\\
&\quad + 8k_1 \cdot k_2 C_{12}^{(2)} + 16k_1 \cdot k_2 C_{23}^{(2)} + 8k_1 \cdot k_2 C_{33}^{(2)},\\
f_2^{(2)} &= -4m_{\tilde{g}}^2 C_{11}^{(2)} - 8\bar{C}_{35}^{(2)} + 6\epsilon C_{35}^{(2)}\\
&\quad + 8C_{23}^{(2)} k_1 \cdot k_2 + 8C_{33}^{(2)} k_1 \cdot k_2,
\end{aligned}$$

$$
\begin{aligned}
f_3^{(2)} &= 4m_{\tilde{g}}^2 C_0^{(2)} - 4m_{\tilde{g}}^2 C_{12}^{(2)} + 8\bar{C}_{24}^{(2)} \\
&\quad -6\epsilon C_{24}^{(2)} - 8\bar{C}_{36}^{(2)} + 6\epsilon C_{36}^{(2)} \\
&\quad +8k_1\cdot k_2 C_{22}^{(2)} + 8k_1\cdot k_2 C_{34}^{(2)}, \\
f_4^{(2)} &= -4m_{\tilde{g}}^2 C_0^{(2)} - 4m_{\tilde{g}}^2 C_{12}^{(2)} - 8\bar{C}_{24}^{(2)} \\
&\quad +6\epsilon C_{24}^{(2)} - 8\bar{C}_{36}^{(2)} + 6\epsilon C_{36}^{(2)} \\
&\quad +8k_1\cdot k_2 C_{12}^{(2)} + 8k_1\cdot k_2 C_{22}^{(2)} + 8k_1\cdot k_2 C_{23}^{(2)} \\
&\quad +8k_1\cdot k_2 C_{34}^{(2)}, \\
f_5^{(2)} &= -8C_{12}^{(2)} - 24C_{23}^{(2)} - 16C_{33}^{(2)}, \\
f_6^{(2)} &= -8C_{12}^{(2)} - 16C_{22}^{(2)} - 8C_{23}^{(2)} - 16C_{34}^{(2)}.
\end{aligned}
\tag{B.4}
$$

Similarly, the $gtt$ vertex functions are composed of left-handed and right-handed contributions plus a counterterm (we define $a$ as the color index of the external gluon and $i,j$ as colors of external top quarks):

$$
\begin{aligned}
\Lambda^a_{\mu,(ij)}(p_1,p_2) &= -\tfrac{g_s\hat{g}_s^2}{16\pi^2}T^a_{ij}\{(2C_{\rm F}-C_{\rm A})(\Lambda_\mu^{(1{\rm L})}(p_1,p_2)P_{\rm L} \\
&\quad +\Lambda_\mu^{(1{\rm R})}(p_1,p_2)P_{\rm R}) \\
&\quad +C_{\rm A}(\Lambda_\mu^{(2{\rm L})}(p_1,p_2)P_{\rm L} \\
&\quad +\Lambda_\mu^{(2{\rm R})}(p_1,p_2)P_{\rm R})\} \\
&\quad +(m_{\tilde{t}_1}\to m_{\tilde{t}_2}, x_i\to y_i)+\Lambda_\mu^{({\rm CT})}.
\end{aligned}
\tag{B.5}
$$

The expressions for $\Lambda_\mu^{(n)}, n = 1{\rm L}, 1{\rm R}, 2{\rm L}, 2{\rm R}$ are given as:

$$
\begin{aligned}
\Lambda_\mu^{(n)}(p_1,p_2) &= h_1^{(n)}\gamma_\mu + h_2^{(n)}p_{1\mu} + h_3^{(n)}p_{2\mu} + h_4^{(n)}\not{p}_1 p_{1\mu} \\
&\quad +h_5^{(n)}\not{p}_1 p_{2\mu} + h_6^{(n)}\not{p}_2 p_{1\mu} \\
&\quad +h_7^{(n)}\not{p}_2 p_{2\mu} + h_8^{(n)}\gamma_\mu\not{p}_1 \\
&\quad +h_9^{(n)}\gamma_\mu\not{p}_2 + +h_{10}^{(n)}\gamma_\mu\not{p}_1\not{p}_2.
\end{aligned}
\tag{B.6}
$$

We define

$$
C_0^{(3)}, C_{ij}^{(3)} = C_0, C_{ij}[-p_1, -p_2, m_{\tilde{t}_1}, m_{\tilde{g}}, m_{\tilde{t}_1}]
$$

and

$$
C_0^{(4)}, C_{ij}^{(4)} = C_0, C_{ij}[-p_1, -p_2, m_{\tilde{g}}, m_{\tilde{t}_1}, m_{\tilde{g}}].
$$

Then we arrive at $h_i^{(n)}$ as follows ($i = 1, 2, \cdots, 10$):

$$
\begin{aligned}
h_1^{(1{\rm L})} &= -2x_2x_4C_{24}^{(3)}, \\
h_2^{(1{\rm L})} &= x_2x_3m_{\tilde{g}}(C_0^{(3)} + 2C_{11}^{(3)}), \\
h_3^{(1{\rm L})} &= x_2x_3m_{\tilde{g}}(C_0^{(3)} + 2C_{12}^{(3)}), \\
h_4^{(1{\rm L})} &= x_2x_4(C_0^{(3)} + 3C_{11}^{(3)} + 2C_{21}^{(3)}), \\
h_5^{(1{\rm L})} &= x_2x_4(C_0^{(3)} + C_{11}^{(3)} + 2C_{12}^{(3)} + 2C_{23}^{(3)}), \\
h_6^{(1{\rm L})} &= x_2x_4(C_{12}^{(3)} + 2C_{23}^{(3)}), \\
h_7^{(1{\rm L})} &= x_2x_4(C_{12}^{(3)} + 2C_{22}^{(3)}), \\
h_8^{(1{\rm L})} &= h_9^{(1{\rm L})} = h_{10}^{(1{\rm L})} = 0
\end{aligned}
\tag{B.7}
$$

and

$$
\begin{aligned}
h_1^{(2{\rm L})} &= x_2x_4(-m_{\tilde{g}}^2C_0^{(4)} - 2C_{24}^{(4)} + \epsilon C_{24}^{(4)}) \\
&\quad +x_2x_4p_1^2(C_{11}^{(4)} + C_{21}^{(4)}) + 2x_2x_4p_1\dot{p}_2(C_{12}^{(4)} + C_{23}^{(4)}) \\
&\quad +x_2x_4p_2^2(C_{12}^{(4)} + C_{22}^{(4)}), \\
h_2^{(2{\rm L})} &= 2x_2x_3m_{\tilde{g}}^2C_{11}^{(4)}, \\
h_3^{(2{\rm L})} &= 2x_2x_3m_{\tilde{g}}^2C_{12}^{(4)}, \\
h_4^{(2{\rm L})} &= -2x_2x_4(C_{11}^{(4)} + C_{21}^{(4)}), \\
h_5^{(2{\rm L})} &= -2x_2x_4(C_{12}^{(4)} + C_{23}^{(4)}), \\
h_6^{(2{\rm L})} &= -2x_2x_4(C_{11}^{(4)} + C_{23}^{(4)}), \\
h_7^{(2{\rm L})} &= -2x_2x_4(C_{12}^{(4)} + C_{22}^{(4)}), \\
h_8^{(2{\rm L})} &= h_9^{(2{\rm L})} = x_2x_3m_{\tilde{g}}^2C_0^{(4)}, \\
h_{10}^{(2{\rm L})} &= x_2x_4(C_{11}^{(4)} - C_{12}^{(4)}).
\end{aligned}
\tag{B.8}
$$

$h_i^{(1{\rm R})}$ and $h_i^{(2{\rm R})}$ can be obtained by exchanging $x_1 \leftrightarrow x_2$ and $x_3 \leftrightarrow x_4$ in $h_i^{(1{\rm L})}$ and $h_i^{(2{\rm L})}$ ($i = 1, 2, \cdots, 10$).

The counterterms are given by:

$$
\begin{aligned}
\Lambda_\mu^{({\rm CT})} &= -C_{\rm F}\tfrac{g_s}{2}T^a_{ij}\gamma_\mu\Big[(\delta Z_{\rm L} + \delta Z_{\rm L}^\dagger)P_{\rm L} \\
&\quad +(\delta Z_{\rm R} + \delta Z_{\rm R}^\dagger)P_{\rm R}\Big].
\end{aligned}
\tag{B.9}
$$

The wave-function renormalization constants can be obtained from (3.3.12) and (3.3.13).

## C. Box corrections

Finally, we list the four form factors $F_{\mu\nu}^{ti}$ as given in (3.5.1) in terms of Passarino–Veltman functions. First we define $F_k^{ti{\rm L}}$ and $F_k^{ti{\rm R}}$ by:

$$
\begin{aligned}
F_{\mu\nu}^{(ti)} &= \tfrac{i\hat{g}_s^2}{16\pi^2}P_{\rm R}[\gamma_\mu\gamma_\nu F_1^{(ti{\rm R})} + \gamma_\nu\gamma_\mu F_2^{(ti{\rm R})} \\
&\quad +p_{1\nu}\gamma_\mu F_3^{(ti{\rm R})} + p_{2\nu}\gamma_\mu F_4^{(ti{\rm R})} \\
&\quad +p_{1\mu}\gamma_\nu F_5^{(ti{\rm R})} + p_{2\mu}\gamma_\nu F_6^{(ti{\rm R})} \\
&\quad +\gamma_\mu\gamma_\nu\not{k}_1 F_7^{(ti{\rm R})} + \gamma_\nu\gamma_\mu\not{k}_1 F_8^{(ti{\rm R})} \\
&\quad +\not{k}_1 p_{1\mu}p_{2\nu}F_9^{(ti{\rm R})} + \not{k}_1 p_{2\mu}p_{1\nu}F_{10}^{(ti{\rm R})} \\
&\quad +\gamma_\mu\not{k}_1 p_{1\nu}F_{11}^{(ti{\rm R})} + \gamma_\mu\not{k}_1 p_{2\nu}F_{12}^{(ti{\rm R})} \\
&\quad +\gamma_\nu\not{k}_1 p_{1\mu}F_{13}^{(ti{\rm R})} + \gamma_\nu\not{k}_1 p_{2\mu}F_{14}^{(ti{\rm R})} \\
&\quad +p_{1\mu}p_{2\nu}F_{15}^{(ti{\rm R})} + p_{1\mu}p_{1\nu}F_{16}^{(ti{\rm R})} \\
&\quad +p_{2\mu}p_{1\nu}F_{17}^{(ti{\rm R})} + \not{k}_1 p_{1\mu}p_{1\nu}F_{18}^{(ti{\rm R})} \\
&\quad +\not{k}_1 p_{2\mu}p_{2\nu}F_{19}^{(ti{\rm R})} + p_{2\mu}p_{2\nu}F_{20}^{(ti{\rm R})}] \\
&\quad +(P_{\rm R}\to P_{\rm L}, F_k^{(ti{\rm R})}\to F_k^{(ti{\rm L})}), \\
&\qquad (k = 1\text{–}20,\ i = 1\text{–}4).
\end{aligned}
\tag{C.1}
$$

In the following we only give the expressions for $F_k^{ti{\rm R}}$ ($k = 1, 2, \cdots, 20$ and $i = 1$–$4$). The expressions for $F_k^{ti{\rm L}}$ can be obtained from $F_k^{ti{\rm R}}$ by exchanging $x_1 \leftrightarrow x_2$ and

$x_3 \leftrightarrow x_4$. Furthermore, the form factors in the $u$-channel are given by

$$F_{\mu\nu}^{(ui)}(k_1,k_2,p_1,p_2) = F_{\nu\mu}^{(ti)}(k_2,k_1,p_1,p_2). \tag{C.2}$$

The expressions of $F_k^{(t1\mathrm{R})}$ $(k = 1\text{–}20)$ are as given below:

$$\begin{aligned} F_1^{(t1\mathrm{R})} &= F_2^{(t1\mathrm{R})} \\ &= -2x_1x_4m_{\tilde{g}}D_{27}^{(1)} + 2x_2x_4m_tD_{311}^{(1)} \\ &\quad +2(x_1x_3 - x_2x_4)m_tD_{313}^{(1)}, \end{aligned} \tag{C.3}$$

$$F_3^{(t1\mathrm{R})} = 4x_1x_3(D_{311}^{(1)} - D_{312}^{(1)}),$$

$$F_4^{(t1\mathrm{R})} = -4x_1x_3(D_{27}^{(1)} + D_{312}^{(1)}),$$

$$F_5^{(t1\mathrm{R})} = 4x_1x_3(D_{27}^{(1)} + D_{311}^{(1)} - D_{313}^{(1)}),$$

$$F_6^{(t1\mathrm{R})} = -4x_1x_3D_{313}^{(1)},$$

$$F_7^{(t1\mathrm{R})} = F_8^{(t1\mathrm{R})} = 2x_1x_3(D_{313}^{(1)} - D_{312}^{(1)}),$$

$$\begin{aligned} F_9^{(t1\mathrm{R})} &= 4x_1x_3(D_{13}^{(1)} - D_{12}^{(1)} - D_{22}^{(1)} - D_{23}^{(1)} - D_{24}^{(1)} \\ &\quad +D_{25}^{(1)} + 2D_{26}^{(1)} - D_{36}^{(1)} + D_{38}^{(1)} - D_{39}^{(1)} + D_{310}^{(1)}), \end{aligned}$$

$$F_{10}^{(t1\mathrm{R})} = 4x_1x_3(D_{37}^{(1)} - D_{39}^{(1)} + D_{38}^{(1)} - D_{310}^{(1)}),$$

$$F_{11}^{(t1\mathrm{R})} = F_{12}^{(t1\mathrm{R})} = F_{13}^{(t1\mathrm{R})} = F_{14}^{(t1\mathrm{R})} = 0,$$

$$\begin{aligned} F_{15}^{(t1\mathrm{R})} &= 4x_1x_3m_t(D_{13}^{(1)} - D_{23}^{(1)} + D_{25}^{(1)} \\ &\quad +D_{26}^{(1)} - D_{39}^{(1)} + D_{310}^{(1)}) \\ &\quad -4x_1x_4m_{\tilde{g}}(D_0^{(1)} + D_{11}^{(1)} + D_{12}^{(1)} \\ &\quad -D_{13}^{(1)} + D_{24}^{(1)} - D_{26}^{(1)}) \\ &\quad +4x_2x_4m_t(D_{11}^{(1)} - D_{13}^{(1)} + D_{21}^{(1)} \\ &\quad +D_{23}^{(1)} + D_{24}^{(1)} - 2D_{25}^{(1)} \\ &\quad -D_{26}^{(1)} + D_{34}^{(1)} + D_{39}^{(1)} - 2D_{310}^{(1)}), \end{aligned}$$

$$\begin{aligned} F_{16}^{(t1\mathrm{R})} &= 4x_1x_3m_t(-D_{25}^{(1)} + D_{26}^{(1)} - D_{35}^{(1)} \\ &\quad +D_{37}^{(1)} - D_{39}^{(1)} + D_{310}^{(1)}) \\ &\quad +4x_1x_4m_{\tilde{g}}(D_{11}^{(1)} - D_{12}^{(1)} + D_{21}^{(1)} \\ &\quad -D_{24}^{(1)} - D_{25}^{(1)} + D_{26}^{(1)}) \\ &\quad -4x_2x_4m_t(D_{21}^{(1)} - D_{24}^{(1)} - D_{25}^{(1)} + D_{26}^{(1)} + D_{31}^{(1)} \\ &\quad -D_{34}^{(1)} - 2D_{35}^{(1)} + D_{37}^{(1)} - D_{39}^{(1)} + 2D_{310}^{(1)}), \end{aligned}$$

$$\begin{aligned} F_{17}^{(t1\mathrm{R})} &= 4x_1x_3m_t(D_{37}^{(1)} - D_{39}^{(1)}) - 4x_1x_4m_{\tilde{g}}(D_{25}^{(1)} - D_{26}^{(1)}) \\ &\quad +4x_2x_4m_t(D_{35}^{(1)} - D_{37}^{(1)} + D_{39}^{(1)} - D_{310}^{(1)}), \end{aligned}$$

$$\begin{aligned} F_{18}^{(t1\mathrm{R})} &= 4x_1x_3(-D_{22}^{(1)} + D_{24}^{(1)} - D_{25}^{(1)} + D_{26}^{(1)} + D_{34}^{(1)} \\ &\quad -D_{35}^{(1)} - D_{36}^{(1)} + D_{37}^{(1)} + D_{38}^{(1)} - D_{39}^{(1)}), \end{aligned}$$

$$F_{19}^{(t1\mathrm{R})} = 4x_1x_3(-D_{23}^{(1)} + D_{26}^{(1)} - D_{39}^{(1)} + D_{38}^{(1)}),$$

$$\begin{aligned} F_{20}^{(t1\mathrm{R})} &= 4x_1x_3m_t(-D_{23}^{(1)} - D_{39}^{(1)}) \\ &\quad +4x_1x_4m_{\tilde{g}}(D_{13}^{(1)} + D_{26}^{(1)}) \\ &\quad +4x_2x_4m_t(D_{23}^{(1)} - D_{25}^{(1)} + D_{39}^{(1)} - D_{310}^{(1)}), \end{aligned}$$

where we denote $D_i^{(1)}, D_{ij}^{(1)}, D_{ijk}^{(1)} = D_i, D_{ij}, D_{ijk}[-p_1, k_1, k_2, m_{\tilde{g}}, m_{\tilde{t_1}}, m_{\tilde{t_1}}, m_{\tilde{t_1}}]$.

The expressions for $F_k^{(t2\mathrm{R})}$ $(k = 1\text{–}20)$ are as follows:

$$\begin{aligned} F_1^{(t2\mathrm{R})} &= 2x_1x_3m_t(D_{27}^{(2)} + D_{313}^{(2)}) + 2x_1x_4m_{\tilde{g}}D_{27}^{(2)} \\ &\quad -2x_2x_4m_t(D_{27}^{(2)} + D_{311}^{(2)}), \end{aligned} \tag{C.4}$$

$$F_2^{(t2\mathrm{R})} = 2x_1x_3m_tD_{313}^{(2)} + 2x_1x_4m_{\tilde{g}}D_{27}^{(2)} - 2x_2x_4m_tD_{311}^{(2)},$$

$$F_3^{(t2\mathrm{R})} = 4x_1x_3(-D_{27}^{(2)} - D_{311}^{(2)} + D_{312}^{(2)}),$$

$$F_4^{(t2\mathrm{R})} = 4x_1x_3(D_{312}^{(2)} - D_{313}^{(2)}),$$

$$\begin{aligned} F_5^{(t2\mathrm{R})} &= 8x_1x_3(D_{27}^{(2)} + D_{311}^{(2)}) + 2x_1x_3m_{\tilde{g}}^2(D_0^{(2)} + D_{11}^{(2)}) \\ &\quad +2x_1x_3m_t^2(-D_{11}^{(2)} - D_{13}^{(2)} - 2D_{21}^{(2)} - D_{23}^{(2)} \\ &\quad -D_{25}^{(2)} - D_{31}^{(2)} - D_{37}^{(2)}) \\ &\quad +2(x_2x_3 + x_1x_4)m_{\tilde{g}}m_t(D_0^{(2)} + D_{11}^{(2)}) \\ &\quad -2x_2x_4m_t^2(D_{11}^{(2)} - D_{13}^{(2)} + D_{21}^{(2)} - D_{25}^{(2)}) \\ &\quad +4x_1x_3k_1\cdot p_1(D_{12}^{(2)} + 2D_{24}^{(2)} + D_{34}^{(2)}) \\ &\quad +4x_1x_3k_1\cdot p_2(D_{13}^{(2)} + D_{25}^{(2)} + D_{26}^{(2)} + D_{310}^{(2)}) \\ &\quad -4x_1x_3p_1\cdot p_2(D_{13}^{(2)} + 2D_{25}^{(2)} + D_{35}^{(2)}), \end{aligned}$$

$$\begin{aligned} F_6^{(t2\mathrm{R})} &= 2x_1x_3m_{\tilde{g}}^2D_{13}^{(2)} \\ &\quad -2x_1x_3m_t^2(D_{23}^{(2)} + D_{25}^{(2)} + D_{33}^{(2)} + D_{35}^{(2)}) \\ &\quad +2(x_2x_3 + x_1x_4)m_{\tilde{g}}m_tD_{13}^{(2)} \\ &\quad +2x_2x_4m_t^2(D_{23}^{(2)} - D_{25}^{(2)}) \\ &\quad +4x_1x_3k_1\cdot p_1(D_{26}^{(2)} + D_{310}^{(2)}) \\ &\quad +4x_1x_3k_1\cdot p_2(D_{23}^{(2)} + D_{39}^{(2)}) \\ &\quad -4x_1x_3p_1\cdot p_2(D_{23}^{(2)} + D_{37}^{(2)}) \\ &\quad +8x_1x_3D_{313}^{(2)}, \end{aligned}$$

$$F_7^{(t2\mathrm{R})} = 2x_1x_3(D_{27}^{(2)} + D_{312}^{(2)}),$$

$$F_8^{(t2\mathrm{R})} = 2x_1x_3D_{312}^{(2)},$$

$$\begin{aligned} F_9^{(t2\mathrm{R})} &= 4x_1x_3(D_{12}^{(2)} - D_{13}^{(2)} + D_{22}^{(2)} + D_{24}^{(2)} - D_{25}^{(2)} \\ &\quad -D_{26}^{(2)} + D_{36}^{(2)} - D_{310}^{(2)}), \end{aligned}$$

$$F_{10}^{(t2\mathrm{R})} = 4x_1x_3(D_{38}^{(2)} - D_{310}^{(2)}),$$

$$F_{11}^{(t2\mathrm{R})} = F_{12}^{(t2\mathrm{R})} = 0,$$

$$\begin{aligned} F_{13}^{(t2\mathrm{R})} &= 2x_1x_3m_t(-D_{12}^{(2)} + D_{13}^{(2)} - D_{24}^{(2)} + D_{25}^{(2)}) \\ &\quad +2x_1x_4m_{\tilde{g}}(D_0^{(2)} + D_{11}^{(2)}) \\ &\quad -2x_2x_4m_t(D_{11}^{(2)} - D_{12}^{(2)} + D_{21}^{(2)} - D_{24}^{(2)}), \end{aligned}$$

$$\begin{aligned} F_{14}^{(t2\mathrm{R})} &= 2x_1x_3m_t(D_{23}^{(2)} - D_{26}^{(2)}) \\ &\quad +2x_1x_4m_{\tilde{g}}D_{13}^{(2)} \\ &\quad -2x_2x_4m_t(D_{25}^{(2)} - D_{26}^{(2)}), \end{aligned}$$

$$
\begin{aligned}
F_{15}^{(t2\mathrm{R})} = {} & 4x_1x_3m_t(D_{12}^{(2)} - D_{13}^{(2)} - D_{23}^{(2)} + D_{24}^{(2)} - D_{25}^{(2)} \\
& + D_{26}^{(2)} - D_{37}^{(2)} + D_{310}^{(2)}) \\
& + 4x_1x_4m_{\tilde{g}}(D_{12}^{(2)} - D_{13}^{(2)} + D_{24}^{(2)} - D_{25}^{(2)}) \\
& - 4x_2x_4m_t(D_{12}^{(2)} - D_{13}^{(2)} + 2D_{24}^{(2)} \\
& - 2D_{25}^{(2)} + D_{34}^{(2)} - D_{35}^{(2)}),
\end{aligned}
$$

$$
\begin{aligned}
F_{16}^{(t2\mathrm{R})} = {} & 4x_1x_3m_t(D_{12}^{(2)} - D_{13}^{(2)} + D_{24}^{(2)} - 2D_{25}^{(2)} \\
& + D_{26}^{(2)} - D_{35}^{(2)} + D_{310}^{(2)}) \\
& + 4x_1x_4m_{\tilde{g}}(-D_0^{(2)} - 2D_{11}^{(2)} \\
& + D_{12}^{(2)} - D_{21}^{(2)} + D_{24}^{(2)}) \\
& + 4x_2x_4m_t(D_{11}^{(2)} - D_{12}^{(2)} + 2D_{21}^{(2)} \\
& - 2D_{24}^{(2)} + D_{31}^{(2)} - D_{34}^{(2)}),
\end{aligned}
$$

$$
\begin{aligned}
F_{17}^{(t2\mathrm{R})} = {} & 4x_1x_3m_t(-D_{23}^{(2)} + D_{26}^{(2)} - D_{37}^{(2)} + D_{39}^{(2)}) \\
& + 4x_1x_4m_{\tilde{g}}(-D_{13}^{(2)} - D_{25}^{(2)} + D_{26}^{(2)}) \\
& + 4x_2x_4m_t(D_{25}^{(2)} - D_{26}^{(2)} + D_{35}^{(2)} - D_{310}^{(2)}),
\end{aligned}
$$

$$
F_{18}^{(t2\mathrm{R})} = 4x_1x_3(D_{22}^{(2)} - D_{24}^{(2)} - D_{34}^{(2)} + D_{36}^{(2)}),
$$

$$
F_{19}^{(t2\mathrm{R})} = 4x_1x_3(-D_{23}^{(2)} + D_{26}^{(2)} + D_{38}^{(2)} - D_{39}^{(2)}),
$$

$$
\begin{aligned}
F_{20}^{(t2\mathrm{R})} = {} & 4x_1x_3m_t(-D_{23}^{(2)} + D_{26}^{(2)} - D_{33}^{(2)} + D_{39}^{(2)}) \\
& + 4x_1x_4m_{\tilde{g}}(-D_{23}^{(2)} + D_{26}^{(2)}) \\
& + 4x_2x_4m_t(D_{23}^{(2)} - D_{26}^{(2)} + D_{37}^{(2)} - D_{310}^{(2)}),
\end{aligned}
$$

where $D_i^{(2)}, D_{ij}^{(2)}, D_{ijk}^{(2)} = D_i, D_{ij}, D_{ijk}[-p_1, k_1, -p_2, m_{\tilde{g}}, m_{\tilde{t_1}}, m_{\tilde{t_1}}, m_{\tilde{g}}]$.

The expressions for $F_k^{(t3\mathrm{R})}$ ($k = 1$–$20$) are written as:

$$
\begin{aligned}
F_1^{(t3\mathrm{R})} = {} & 2x_1x_3m_t(D_{27}^{(3)} + 2D_{313}^{(3)}) \\
& + x_1x_3m_tm_{\tilde{g}}^2(D_0^{(3)} + D_{13}^{(3)}) \\
& - x_1x_3m_t^3(D_0^{(3)} + 2D_{11}^{(3)} - D_{13}^{(3)} + D_{21}^{(3)} \\
& + 2D_{33}^{(3)} + 2D_{35}^{(3)} - 2D_{37}^{(3)}) \\
& + 2x_1x_4m_{\tilde{g}}D_{27}^{(3)} + x_1x_4m_{\tilde{g}}^3D_0^{(3)} \\
& - x_1x_4m_t^2m_{\tilde{g}}(D_0^{(3)} + 2D_{11}^{(3)} - 2D_{13}^{(3)} \\
& + D_{21}^{(3)} + 2D_{23}^{(3)} - 2D_{25}^{(3)}) \\
& + 2x_2x_4m_t(D_{27}^{(3)} + 2D_{311}^{(3)} - 2D_{313}^{(3)}) \\
& + x_2x_4m_tm_{\tilde{g}}^2(D_{11}^{(3)} - D_{13}^{(3)}) \\
& - x_2x_4m_t^3(D_{11}^{(3)} - D_{13}^{(3)} + 2D_{21}^{(3)} + 2D_{23}^{(3)} - 4D_{25}^{(3)} \\
& + D_{31}^{(3)} - 2D_{33}^{(3)} - 3D_{35}^{(3)} + 4D_{37}^{(3)}) \\
& + 2x_1x_3m_tk_1 \cdot p_1(D_{12}^{(3)} - D_{13}^{(3)} - D_{23}^{(3)} + D_{24}^{(3)} \\
& + D_{33}^{(3)} - D_{37}^{(3)} - D_{39}^{(3)} + D_{310}^{(3)}) \\
& + 2x_1x_4m_{\tilde{g}}k_1 \cdot p_1(D_{11}^{(3)} + D_{12}^{(3)} - 2D_{13}^{(3)} \\
& + D_{23}^{(3)} + D_{24}^{(3)} - D_{25}^{(3)} - D_{26}^{(3)}) \\
& + 2x_2x_4m_tk_1 \cdot p_1(D_{11}^{(3)} - D_{13}^{(3)} + D_{21}^{(3)} + 2D_{23}^{(3)} \\
& + D_{24}^{(3)} - 3D_{25}^{(3)} - D_{26}^{(3)} - D_{33}^{(3)} + D_{34}^{(3)} - D_{35}^{(3)} \\
& + 2D_{37}^{(3)} + D_{39}^{(3)} - 2D_{310}^{(3)}) \\
& + 2x_1x_3m_tk_1 \cdot p_2(-D_{13}^{(3)} - D_{26}^{(3)} + D_{33}^{(3)} - D_{39}^{(3)}) \\
& + 2x_1x_4m_{\tilde{g}}k_1 \cdot p_2(-D_{13}^{(3)} + D_{23}^{(3)} - D_{26}^{(3)}) \\
& + 2x_2x_4m_tk_1 \cdot p_2(D_{23}^{(3)} - D_{25}^{(3)} - D_{33}^{(3)} + D_{37}^{(3)} \\
& + D_{39}^{(3)} - D_{310}^{(3)}) \\
& + 2x_1x_3m_tp_1 \cdot p_2(D_{13}^{(3)} + D_{25}^{(3)} - D_{33}^{(3)} + D_{37}^{(3)}) \\
& + 2x_1x_4m_{\tilde{g}}p_1 \cdot p_2(D_{13}^{(3)} - D_{23}^{(3)} + D_{25}^{(3)}) \\
& + 2x_2x_4m_tp_1 \cdot p_2(-D_{23}^{(3)} + D_{25}^{(3)} + D_{33}^{(3)} \\
& + D_{35}^{(3)} - D_{37}^{(3)}),
\end{aligned}
\tag{C.5}
$$

$$
\begin{aligned}
F_2^{(t3\mathrm{R})} = {} & -2x_1x_4m_{\tilde{g}}D_{27}^{(3)} - 2x_1x_3m_tD_{313}^{(3)} \\
& - 2x_2x_4m_t(D_{27}^{(3)} + D_{311}^{(3)} - D_{313}^{(3)}),
\end{aligned}
$$

$$
\begin{aligned}
F_3^{(t3\mathrm{R})} = {} & 4x_1x_3(D_{27}^{(3)} + 2D_{311}^{(3)} + D_{312}^{(3)} - 3D_{313}^{(3)}) \\
& + 2x_1x_3m_{\tilde{g}}^2(-D_0^{(3)} + D_{11}^{(3)} - D_{13}^{(3)}) \\
& + 2x_1x_3m_t^2(D_{13}^{(3)} - D_{21}^{(3)} + 2D_{25}^{(3)} - D_{31}^{(3)} \\
& + 2D_{33}^{(3)} + 3D_{35}^{(3)} - 4D_{37}^{(3)}) \\
& - 2x_2x_3m_tm_{\tilde{g}}D_0^{(3)} - 2x_1x_4m_tm_{\tilde{g}}D_0^{(3)} \\
& - 2x_2x_4m_t^2(D_0^{(3)} + D_{11}^{(3)}) \\
& + 4x_1x_3k_1 \cdot p_1(D_{23}^{(3)} + D_{24}^{(3)} - D_{25}^{(3)} - D_{26}^{(3)} \\
& - D_{33}^{(3)} + D_{34}^{(3)} - D_{35}^{(3)} + 2D_{37}^{(3)} + D_{39}^{(3)} - 2D_{310}^{(3)}) \\
& + 4x_1x_3k_1 \cdot p_2(-D_{25}^{(3)} + D_{26}^{(3)} - D_{33}^{(3)} \\
& + D_{37}^{(3)} + D_{39}^{(3)} - D_{310}^{(3)}) \\
& + 4x_1x_3p_1 \cdot p_2(D_{33}^{(3)} + D_{35}^{(3)} - 2D_{37}^{(3)}),
\end{aligned}
$$

$$
\begin{aligned}
F_4^{(t3\mathrm{R})} &= 4x_1x_3D_{312}^{(3)} - 2x_1x_3m_{\tilde{g}}^2D_0^{(3)} \\
&+2x_1x_3m_t^2(D_{11}^{(3)} + D_{21}^{(3)} + 2D_{23}^{(3)} - 2D_{25}^{(3)}) \\
&-2x_2x_3m_tm_{\tilde{g}}D_0^{(3)} - 2x_1x_4m_tm_{\tilde{g}}D_0^{(3)} \\
&-2x_2x_4m_t^2(D_0^{(3)} + D_{11}^{(3)}) \\
&+4x_1x_3k_1\cdot p_1(-D_{23}^{(3)} + D_{25}^{(3)}) \\
&+4x_1x_3k_1\cdot p_2(-D_{23}^{(3)} + D_{26}^{(3)}) \\
&+4x_1x_3p_1\cdot p_2(D_{23}^{(3)} - D_{25}^{(3)}),
\end{aligned}
$$

$$
\begin{aligned}
F_5^{(t3\mathrm{R})} &= 4x_1x_3(-D_{311}^{(3)} + D_{313}^{(3)}) + 2x_1x_3m_{\tilde{g}}^2D_0^{(3)} \\
&-2x_1x_3m_t^2(D_{13}^{(3)} + D_{25}^{(3)}) \\
&+2x_2x_3m_tm_{\tilde{g}}(D_0^{(3)} + D_{11}^{(3)} - D_{13}^{(3)}) \\
&+2x_1x_4m_tm_{\tilde{g}}(D_0^{(3)} + D_{11}^{(3)} - D_{13}^{(3)}) \\
&+2x_2x_4m_t^2(D_0^{(3)} + 2D_{11}^{(3)} - D_{13}^{(3)} + D_{21}^{(3)} - D_{25}^{(3)}) \\
&+4x_1x_3k_1\cdot p_2(D_{25}^{(3)} - D_{26}^{(3)}),
\end{aligned}
$$

$$
\begin{aligned}
F_6^{(t3\mathrm{R})} &= -8x_1x_3D_{313}^{(3)} - 2x_1x_3m_{\tilde{g}}^2D_{13}^{(3)} \\
&+2x_1x_3m_t^2(D_{25}^{(3)} + 2D_{33}^{(3)} + D_{35}^{(3)} - 2D_{37}^{(3)}) \\
&-2x_2x_3m_tm_{\tilde{g}}D_{13}^{(3)} \\
&-2x_1x_4m_tm_{\tilde{g}}D_{13}^{(3)} - 2x_2x_4m_t^2(D_{13}^{(3)} + D_{25}^{(3)}) \\
&+4x_1x_3k_1\cdot p_1(D_{23}^{(3)} - D_{25}^{(3)} - D_{33}^{(3)} \\
&+D_{37}^{(3)} + D_{39}^{(3)} - D_{310}^{(3)}) \\
&+4x_1x_3k_1\cdot p_2(-D_{33}^{(3)} + D_{39}^{(3)}) \\
&+4x_1x_3p_1\cdot p_2(D_{33}^{(3)} - D_{37}^{(3)}),
\end{aligned}
$$

$$
\begin{aligned}
F_7^{(t3\mathrm{R})} &= -4x_1x_3(D_{312}^{(3)} - D_{313}^{(3)}) \\
&+x_1x_3m_{\tilde{g}}^2(D_0^{(3)} - D_{12}^{(3)} + D_{13}^{(3)}) \\
&+x_1x_3m_t^2(-D_{11}^{(3)} + D_{12}^{(3)} - D_{13}^{(3)} - D_{21}^{(3)} \\
&+2D_{24}^{(3)} - 2D_{26}^{(3)} - 2D_{33}^{(3)} + D_{34}^{(3)} - D_{35}^{(3)} \\
&+2D_{37}^{(3)} + 2D_{39}^{(3)} - 2D_{310}^{(3)}) \\
&+(x_2x_3 + x_1x_4)m_tm_{\tilde{g}}D_0^{(3)} \\
&+x_2x_4m_t^2(D_0^{(3)} + D_{11}^{(3)}) \\
&+2x_1x_3k_1\cdot p_1(-D_{22}^{(3)} - D_{23}^{(3)} \\
&+2D_{26}^{(3)} + D_{33}^{(3)} - D_{36}^{(3)} \\
&-D_{37}^{(3)} + D_{38}^{(3)} - 2D_{39}^{(3)} + 2D_{310}^{(3)}) \\
&+2x_1x_3k_1\cdot p_2(D_{33}^{(3)} + D_{38}^{(3)} - 2D_{39}^{(3)}) \\
&+2x_1x_3p_1\cdot p_2(D_{25}^{(3)} - D_{26}^{(3)} \\
&-D_{33}^{(3)} + D_{37}^{(3)} + D_{39}^{(3)} - D_{310}^{(3)}),
\end{aligned}
$$

$$
F_8^{(t3\mathrm{R})} = 2x_1x_3(D_{27}^{(3)} + D_{312}^{(3)} - D_{313}^{(3)}),
$$

$$
\begin{aligned}
F_9^{(t3\mathrm{R})} &= 4x_1x_3(D_{22}^{(3)} + D_{23}^{(3)} - D_{25}^{(3)} - D_{26}^{(3)} \\
&+D_{36}^{(3)} - D_{38}^{(3)} + D_{39}^{(3)} - D_{310}^{(3)}),
\end{aligned}
$$

$$
\begin{aligned}
F_{10}^{(t3\mathrm{R})} &= 4x_1x_3(D_{25}^{(3)} - D_{26}^{(3)} - D_{37}^{(3)} \\
&-D_{38}^{(3)} + D_{39}^{(3)} + D_{310}^{(3)}),
\end{aligned}
$$

$$
\begin{aligned}
F_{11}^{(t3\mathrm{R})} &= 2x_1x_3m_t(-D_{25}^{(3)} + D_{26}^{(3)}) \\
&+2x_1x_4m_{\tilde{g}}(-D_{11}^{(3)} + D_{12}^{(3)}) \\
&+2x_2x_4m_t(-D_{11}^{(3)} + D_{12}^{(3)} - D_{21}^{(3)} \\
&+D_{24}^{(3)} + D_{25}^{(3)} - D_{26}^{(3)}),
\end{aligned}
$$

$$
\begin{aligned}
F_{12}^{(t3\mathrm{R})} &= 2x_1x_3m_t(D_{13}^{(3)} + D_{26}^{(3)}) + 2x_1x_4m_{\tilde{g}}D_{12}^{(3)} \\
&+2x_2x_4m_t(D_{12}^{(3)} - D_{13}^{(3)} + D_{24}^{(3)} - D_{26}^{(3)}),
\end{aligned}
$$

$$
\begin{aligned}
F_{13}^{(t3\mathrm{R})} &= 2x_1x_3m_t(D_{12}^{(3)} - D_{13}^{(3)} + D_{24}^{(3)} - D_{26}^{(3)}) \\
&+2x_1x_4m_{\tilde{g}}(D_{11}^{(3)} - D_{13}^{(3)}) \\
&+2x_2x_4m_t(D_{11}^{(3)} - D_{12}^{(3)} \\
&+D_{21}^{(3)} - D_{24}^{(3)} - D_{25}^{(3)} + D_{26}^{(3)}),
\end{aligned}
$$

$$
\begin{aligned}
F_{14}^{(t3\mathrm{R})} &= -2x_1x_3m_t(D_{13}^{(3)} + D_{26}^{(3)}) \\
&-2x_1x_4m_{\tilde{g}}D_{13}^{(3)} \\
&+2x_2x_4m_t(-D_{25}^{(3)} + D_{26}^{(3)}),
\end{aligned}
$$

$$
\begin{aligned}
F_{15}^{(t3\mathrm{R})} &= -4x_1x_3m_t(D_{12}^{(3)} - D_{23}^{(3)} + D_{24}^{(3)} \\
&+D_{25}^{(3)} - D_{39}^{(3)} + D_{310}^{(3)}) \\
&+4x_1x_4m_{\tilde{g}}(-D_{11}^{(3)} - D_{12}^{(3)} \\
&+D_{13}^{(3)} - D_{24}^{(3)} + D_{26}^{(3)}) \\
&+4x_2x_4m_t(-D_{11}^{(3)} + D_{13}^{(3)} \\
&-D_{21}^{(3)} - D_{23}^{(3)} \\
&-D_{24}^{(3)} + 2D_{25}^{(3)} + D_{26}^{(3)} \\
&-D_{34}^{(3)} - D_{39}^{(3)} + 2D_{310}^{(3)}),
\end{aligned}
$$

$$
\begin{aligned}
F_{16}^{(t3\mathrm{R})} &= -4x_1x_3m_t(D_{12}^{(3)} - D_{13}^{(3)} + D_{24}^{(3)} \\
&-D_{25}^{(3)} - D_{35}^{(3)} + D_{37}^{(3)} - D_{39}^{(3)} + D_{310}^{(3)}) \\
&+4x_1x_4m_{\tilde{g}}(-D_{12}^{(3)} + D_{13}^{(3)} + D_{21}^{(3)} \\
&-D_{24}^{(3)} - D_{25}^{(3)} + D_{26}^{(3)}) \\
&+4x_2x_4m_t(D_{21}^{(3)} - D_{24}^{(3)} - D_{25}^{(3)} + D_{26}^{(3)} \\
&+D_{31}^{(3)} - D_{34}^{(3)} - 2D_{35}^{(3)} \\
&+D_{37}^{(3)} - D_{39}^{(3)} + 2D_{310}^{(3)}),
\end{aligned}
$$

$$
\begin{aligned}
F_{17}^{(t3\mathrm{R})} &= 4x_1x_3m_t(D_{13}^{(3)} + D_{26}^{(3)} - D_{37}^{(3)} + D_{39}^{(3)}) \\
&+4x_1x_4m_{\tilde{g}}(D_{13}^{(3)} - D_{25}^{(3)} + D_{26}^{(3)}) \\
&+4x_2x_4m_t(-D_{35}^{(3)} + D_{37}^{(3)} - D_{39}^{(3)} + D_{310}^{(3)}),
\end{aligned}
$$

$$
\begin{aligned}
F_{18}^{(t3\mathrm{R})} &= 4x_1x_3(D_{22}^{(3)} - D_{24}^{(3)} + D_{25}^{(3)} - D_{26}^{(3)} \\
&-D_{34}^{(3)} + D_{35}^{(3)} + D_{36}^{(3)} \\
&-D_{37}^{(3)} - D_{38}^{(3)} + D_{39}^{(3)}),
\end{aligned}
$$

$$
\begin{aligned}
F_{19}^{(t3\mathrm{R})} &= 4x_1x_3(D_{23}^{(3)} - D_{26}^{(3)} \\
&-D_{38}^{(3)} + D_{39}^{(3)}),
\end{aligned}
$$

$$
\begin{aligned}
F_{20}^{(t3\mathrm{R})} &= 4x_1x_3m_t(D_{13}^{(3)} + D_{23}^{(3)} + D_{26}^{(3)} + D_{39}^{(3)}) \\
&+4x_1x_4m_{\tilde{g}}(D_{13}^{(3)} + D_{26}^{(3)}) \\
&+4x_2x_4m_t(-D_{23}^{(3)} + D_{25}^{(3)} - D_{39}^{(3)} + D_{310}^{(3)}),
\end{aligned}
$$

where $D_i^{(3)}, D_{ij}^{(3)}, D_{ijk}^{(3)} = D_i, D_{ij}, D_{ijk}[-p_1, k_1, k_2, m_{\tilde{t_1}}, m_{\tilde{g}}, m_{\tilde{g}}, m_{\tilde{g}}]$.

The $F_k^{(t4\mathrm{R})}$ ($k = 1$–$20$) are written explicitly as:

$$\begin{aligned} F_1^{(t4\mathrm{R})} &= F_2^{(t4\mathrm{R})} \\ &= \tfrac{1}{2}((x_1 x_3 m_t (C_{11} - C_{12}) \\ &\quad + x_2 x_4 m_t C_{12} - x_2 x_3 m_{\tilde{g}} C_0) \\ &\quad [-p_1, p_1 + p_2, m_{\tilde{g}}, m_{\tilde{t}_1}, m_{\tilde{t}_1}]), \end{aligned} \tag{C.6}$$

$$F_i^{(t4\mathrm{R})} = 0, \quad (i = 3, 4, \cdots 20).$$

## References


1. H.E. Haber, G.L. Kane, Phys. Rep. **117**, 75 (1985); J.F. Gunion, H.E. Haber, Nucl. Phys. B **272**, 1 (1986)
2. P.C. Bhat, for the D0 collaboration, talk presented at the Wine and Cheese Seminar at Fermilab, February 1997
3. M. Glück, J.F. Owens, E. Reya, Phys. Rev. D **17**, 2324 (1978); B.L. Combridge, Nucl. Phys. B **151**, 429 (1979); H. Georgi et al., Ann. Phys. (N.Y.) **114**, 273 (1978)
4. P. Nason, S. Dawson, R.K. Ellis, Nucl. Phys. B **303**, 607 (1988); G. Altarelli, M. Diemoz, G. Martinelli, P. Nason, Nucl. Phys. B **308**, 724 (1988); W. Beenakker, H. Kujif, W.L. van Neerven, J. Smith, Phys. Rev. D **40**, 54 (1989)
5. C. Li, B. Hu, J. Yang, C. Hu, Phys. Rev. D **52**, 5014 (1995); Z. Sullivan, hep-ph/9611302
6. H.Y. Zhou, C.S. Li, Phys. Rev. D **55**, 4421 (1997)
7. A. Bartl, E. Christova, W. Majerotto, Nucl. Phys. B **460**, 235 (1996)
8. T. Gehrmann, W.J. Stirling, Z. Phys. C **65**, 461 (1995); S.J. Brodsky, M. Burkardt, I. Schmidt, Nucl. Phys. B **441**, 197 (1995) and the references therein
9. M. Glück, E. Reya, A. Vogt, Z. Phys. C **48**, 471 (1990); M. Glück, E. Reya, A. Vogt, Z. Phys. C **67**, 433 (1995)
10. M. Glück, E. Reya, M. Stratmann, Phys. Rev. D **53**, 4775 (1996)
11. M. Stratmann, hep-ph/9710379
12. S.P. Martin, M.T. Vaughn, Phys. Lett. B **318**, 331 (1993); W. Beenakker, R. Höpker, P.M. Zerwas, Phys. Lett. B **378**, 159 (1996)
13. W. Beenaker, R. Höpker, T. Plehn, P.M. Zerwas, DESY.96-178 (1996)
14. B.A. Kniehl, Phys. Rep. **240**, 211 (1994)
15. G. Passarino, M. Veltman, Nucl. Phys. B **160**, 151 (1979)